Comprehensive Map of the Regulated Cell Death Signaling Network: A Powerful Analytical Tool for Studying Diseases

Jean-Marie Ravel, Luis Cristobal Monraz Gomez, Nicolas Sompairac, Laurence Calzone, Boris Zhivotovsky, Guido Kroemer, Emmanuel Barillot, Andrei Zinovyev, Inna Kuperstein

Comprehensive map of the regulated cell death signalling network: a powerful analytical tool for studying diseases

Jean-Marie Ravel[1-3*], L. Cristobal Monraz Gomez[1*], Nicolas Sompairac[1,4], Laurence Calzone[1], Boris Zhivotovsky[5,6], Guido Kroemer[7-11], Emmanuel Barillot[1], Andrei Zinovyev[1] and Inna Kuperstein[1#]

[1]Institut Curie, 26 rue d'Ulm, F-75005 Paris, France, PSL Research University, F-75005 Paris, France, Inserm, U900, F-75005, Paris France, Mines Paris Tech, F-77305 cedex Fontainebleau, France

[2]Laboratoire de génétique, Centre Régional Hospitalier Universitaire de Nancy, Vandœuvre-lès-Nancy

[3]INSERM UMR 954, Université de Lorraine, Vandœuvre-lès-Nancy

[4]Université Paris Descartes, Centre de Recherches Interdisciplinaires, Paris, France

[5]Faculty of Medicine, Lomonosov Moscow State University, 119991, Moscow, Russia

[6]Division of Toxicology, Institute of Environmental Medicine, Karolinska Institutet, Box 210, 17177, Stockholm, Sweden

[7]Equipe labellisée par la Ligue contre le cancer, Université Paris Descartes, Université Sorbonne Paris Cité, Université Paris Diderot, Sorbonne Université, INSERM U1138, Centre de Recherche des Cordeliers, Paris, France

[8]Metabolomics and Cell Biology Platforms, Institut Gustave Roussy, Villejuif, France

[9]Pôle de Biologie, Hôpital Européen Georges Pompidou, AP-HP, Paris, France

[10]Suzhou Institute for Systems Biology, Chinese Academy of Sciences, Suzhou, China

[11]Karolinska Institute, Department of Women's and Children's Health, Karolinska University Hospital, Stockholm, Sweden

*Equal contribution

[#]Corresponding author

Abstract

The processes leading to, or avoiding cell death are widely studied, because of their frequent perturbation in various diseases. Cell death occurs in three highly interconnected steps: initiation, signalling and execution. We used a systems biology approach to gather information about all known modes of regulated cell death (RCD). Based on the experimental data retrieved from literature by manual curation, we graphically depicted the biological processes involved in RCD in a form of seamless comprehensive signalling network map. The molecular mechanisms of each RCD mode are represented in detail. The RCD network map is divided into 26 functional modules that can be visualized contextually in the whole seamless network, as well as in individual diagrams. The resource is freely available and accessible via several web platforms for map navigation, data integration and analysis. The RCD network map was employed for interpreting the functional differences in cell death regulation between Alzheimer's disease and non-small cell lung cancer based on gene expression data that allowed emphasizing the molecular mechanisms underlying the inverse comorbidity between the two pathologies. In addition, the map was used for the analysis of genomic and transcriptomic data from ovarian cancer patients that provided RCD map-based signatures of four distinct tumor subtypes and highlighted difference in regulations of cell death molecular mechanisms.

Keywords

Regulated cell death, modes of cell death, survival, apoptosis, necroptosis, autophagy, ferroptosis, parthanatos, pyroptosis, signalling network, comprehensive map, process description diagram, pathways, biocuration, NaviCell, MINERVA, NDEx, data visualization, enrichment analysis, module activity, lung cancer, Alzheimer's disease

Introduction

Cell death garners special attention not only because it represents the endpoint of the cell's life cycle, but also because of the molecular machinery leading to cellular demise is perturbed in many different diseases[1,2]. There are two major scenarios sealing a cell's final fate. Cells can either die from regulated cell death (RCD) or succumb to accidental cell death[3,4]. Accidental or non-regulated cell death, which is often referred to as necrosis, is a sudden process that combines cell membrane rupture and release of the cellular content into the surrounding environment[5]. In contrast, RCD involves an active contribution by the cells and may be executed through a panoply of different pathways that include (but are not limited to) apoptosis, necroptosis, autophagy, ferroptosis, parthanatos and pyroptosis[6,7].

One of the most studied modes of RCD is apoptosis, a 'clean' cell elimination process that has been thought to be non-inflammatory and non-immunogenic. However, in specific circumstances, cells dying from apoptosis may induce an immune response against dead-cell antigens[8]. Apoptosis is a highly regulated, energy-dependent process that requires ATP supply and, therefore, hinges on a functional bioenergetics metabolism. The severity of environmental stress, damage, genetic or epigenetic perturbations dictate the choice between survival or death program and also mode of cell death execution, be it apoptosis or another lethal subroutine[9]. A challenge is to integrate all the distinct initiation, signalling and execution pathways into one integrated map. RCD is coordinated by numerous signalling pathways including trophic signals relayed by AKT and mTOR, stress kinase including ERK and JNK, or transcription factors such as NF-κB. RCD is also regulated by mitochondria and glucose metabolism that dictate the energy supply status. In addition, there is a complex post-transcriptional regulation level by non-coding RNAs including miRNAs and post-translational modifications of apoptosis-related proteins. Morphologically, apoptosis is characterized by cell shrinkage, nuclear condensation and fragmentation, cellular detachment from surrounding tissue and surface exposure of 'eat-me' signals such as phosphatidylserine that facilitate removal of the dying cells by macrophages.

Another well-studied form of RCD, autophagy, is activated under various stress situations, in particular in response to a shortage in energy supply in the context of starvation or scarcity of growth factors[10]. Autophagy ensures cell homeostasis by recycling cellular organelles and macromolecules, thereby, mediating cytoprotection and reducing the propensity of cells to undergo RCD. In specific circumstances, however, autophagy can be switched to a process of self-elimination leading to cell death. Necroptosis is a signalling-

mediated mode of cell death with morphological features similar to necrosis. Necroptosis is accompanied by "swelling" of cells and organelles and rapid loss of plasma membrane integrity. Ferroptosis is a cell death modality induced by an accumulation of lipid peroxides due to a dysregulation of iron metabolism that facilitates the generation or reactive oxygen species (ROS) and consequent peroxidation of membrane lipids[11]. Parthanatos is a Poly [ADP-ribose] polymerase 1 (PARP1) dependent cell death mode induced mostly by intracellular inputs such as DNA damage. When activated by single-stranded DNA breaks, PARP1 synthesizes poly (ADP-ribose) chains (PAR) that are covalently attached to nuclear proteins while consuming ADP and NAD+. PAR then acts as an activating signal for other DNA-repairing enzymes. However, in the case of excessive DNA damage, DNA repair processes are overstimulated. This leads to the consumption of ATP and NAD depletion, triggering cellular execution. Finally, parthanatos is associated to mitochondrial fission, its major phenotype[12]. Pyroptosis is a caspase-1 dependent cell death modality that can be activated by extracellular signals (such as bacterial lipopolysaccharide, LPS) that bind to receptors (such as NLRC4), inducing receptor dimerization that triggers PYCARD protein recruitment and thus caspase-1 activation.

This massive knowledge is scattered through thousands of scientific publications. This situation hampers not only the holistic understanding of RCD regulation, but also the application of bioinformatics and systems biology approaches. Efforts of systematic collection and knowledge formalization about molecular interactions in a structured and computer-readable format have already been applied to numerous pathway databases. Several databases contain partially overlapping collections of signalling diagrams representing different modes of cell death, mitochondria and glucose metabolism in some detail[13–17]. However, the limiting factor of this type of signalling representation is the lack of an integrated view of the pathways linking upstream inputs, such as activators of 'death receptor', damaging agents or intracellular stressors to the different regulated cell death modes.

As an additional approach for data formalization, protein-protein interaction (PPI) networks are used for representing reciprocal effects between molecular entities. However, PPI diagrams do not represent interactions between non-protein molecular entities (such as metabolites) and the depth of process description is generally not sufficient to understand the directionality of the signal flow, regulatory effects or feedback circuitries.

Cell signalling can also be depicted at the level of biochemical reactions in the form of process diagrams, thus creating a comprehensive map as it has been done for RB-E2F signalling[18], mTOR signalling[19], Alzheimer's pathogenesis[20], influenza A virus replication[21], the Alas of Cancer Signalling Networks (ACSN)[22] and others[23].

Here, we present the construction of a comprehensive illustration of interactions among different RCD modes in the form of a seamless signalling network. The resulting map constitutes the first integrated representation of all known modes of RCD together. The map depicts inputs, the initiating factors that activate different cell

death mechanisms, the signalling pathways responsible for the choice of distinct lethal subroutines and the final executing mechanisms. These three elements correspond to the three layers of the map. The RCD map also covers related energy, metabolic and mitochondrial mechanisms. In order to facilitate navigation and usage, the map is divided into functional modules. Of note, this systems biology resource is freely available, allows easy navigation and curation by the community, facilitated by several web-based platform such as NaviCell[24], MINERVA[25] and NDEx[26]. Finally, we demonstrated that the RCD map may be used as a powerful tool for comparing cell death regulation in several human diseases.

Results

General characteristics of Regulated Cell Death map

The molecular mechanisms are depicted on the map in the form of biochemical reaction network using a well-established methodology[27]. The diagrams are built using the Systems Biology Graphical Notation language (SBGN)[28] and drawn using the CellDesigner tool[29] that ensures compatibility of the maps with various tools for network analysis, data integration and network modelling. Manual literature curation was carefully performed in several steps, first retrieving a level of well-established 'consensus' information from major reviews and then adding details from recent original publications (Figure 1 and Supplemental Figure 1).

RCD is a tightly regulated process characterized by numerous cross-talks between molecular mechanisms. In order to represent these details in an organized and user-friendly manner, we handled this complexity in two ways. First, the map has a *hierarchical structure* and is constructed around three successive layers (initiation, signalling, execution). The map is also split into meta-modules, then into functional modules, and, ultimately, the most detailed level describes biochemical reactions (Figure 2 and Table 1). The second strategy to address complexity relies on the introduction of a *tagging system* for map layers, modules and each entity and reaction that indicate their involvement in different biological processes. This system allows tracing the participation of entities in different processes and helps to retrieve a backbone structure of the network diagram. Each molecular player and reaction in the maps were annotated in the NaviCell format, including PubMed references, cross-references with other databases, notes by the map manager. In addition, each molecular player and reaction was assigned with a confidence score and tags (Figure 2 and Supplemental Figure 2). The RCD map summarizes information 1008 proteins, 260 genes, 93 miRNAs and 2020 reactions. It is based on 800 original scientific publications. The map is divided into three meta-modules and 26 separate functional modules (Table 1). The principles and procedure for map construction, including the graphical standards, data model, literature curation rules, data input from other databases and the detailed tagging system and confidence scores description, are provided in the STAR Methods section.

Structure of the Regulated Cell Death map

RCD is a dynamic process, wherein the propagation and duration of signals determine cell fate decision. As the name suggests, RCD is highly regulated, in addition, different players may share the same modulators or the

same targets. The RCD process can be split into three major steps, initiation, signalling and execution, which we defined as the *layers of the map* (Figure 2 and Table 1). The "Initiation" layer depicts input signals and mechanisms that ignite RCD.

The three major inputs are grouped into the "Ligand-Receptor", "Metabolism" and "Stress Response" modules. The "Signalling" layer is the level where the decision between cell death and survival is made along with the selection of the cell death mode. It gathers all previously described cell death modes and their inhibition processes. It is also the step of interplay where primary clues transmit their signal to a secondary messenger depending of the cellular context. Thus, the same primary/initiation cue can trigger different types of outcome depending on the absence or presence of other entities. The "Execution" layer represents the final step of RCD in which the process trespasses the point of-no-return and vital components of the cell are irreversibly degraded. Mitochondrial outer membrane permeabilization (MOMP), mitochondrial permeability transition (MPT) and caspases are the major players of this step. Each module in the "signalling" layer triggers specific combination of modules in the "execution" layer. For example, initiation of parthanatos triggers large scale DNA fragmentation, whereas ignition of apoptosis preferentially leads to caspases activation and to MOMP.

In addition, a modular structure of RCD map has been introduced, allowing to explore each molecular mechanism separately, represented as an independent module map. The RCD map is divided into *functional meta-modules* that are further subdivided into smaller functional modules, together creating 26 *functional modules*. For example, the meta-module dealing with "death receptor pathways" contains information on the response to TRAIL, the ligation of Fas receptors, the response to TNF, and the signalling of dependence receptors (Table 1). The detailed description of layers, functional meta-modules and modules is found in the Supplemental item 1.

Contents of the RCD map

The RCD map gathers information on all the major regulated death pathway, thus allowing to illustrate their cross-talks (Figure 3).

Apoptosis is classically divided into *"extrinsic apoptosis"*, depicted at the right of our drawing and *"intrinsic apoptosis"*, at the left[7]. Extrinsic apoptosis is triggered by death receptors, in which ligand binding triggers the signal, and dependence receptors, in which ligand withdrawal activates the signal[30]. This initiation signal leads to rapid activation of caspases (especially CASP3 and CASP7) and eventually apoptotic death[31]. Intrinsic apoptosis preferentially leads to mitochondrial outer membrane permeabilization (MOMP), often as a result of the oligomerization of BAX/BAK[32] and their insertion into the mitochondrial membrane. Apoptosome-dependent CASP9 activation in the cytoplasm occurs as a result of the mitochondrial release of CYCS (previously known as cytochrome *c*) and SMAC (also known as DIABLO). CASP9 activation leads to subsequent proteolytic CASP3 and CASP7 activation and apoptosis (Supplemental Figure 3A).

The *Necroptosis* outbreak is guided by RIPK1 and RIPK3 proteins[33]. When CASP8 is inhibited, especially by c-FLIP (encoded by *CFLAR*), RIPK3 is activated by RIPK1. RIPK3 and MLKL recruitment into the necrosome complex triggers the features of necroptosis (a raise in cytosolic Ca^{2+}, ROS production, PARP1 over-activation, and lysosome membrane permeabilization) and eventually necroptotic death (Supplemental Figure 3B).

Autophagy and lysosome-dependent cell death is influenced by the cell energy status and coupled to the formation of autophagosomes and autophagolysosomes[34]. ROS, amino acid starvation and DNA damage result in a decrease of cytosolic 5' adenosine triphosphate (ATP) and a consequent increase in 5' adenosine monophosphate (AMP), thus triggering activation of the AMP-dependent kinase (AMPK). This triggers (1) inhibition of pro-survival complex mTORC1; (2) activation of BECN1 (Beclin 1) and results in autophagosome formation (Supplemental Figure 3C).

The central feature of *parthanatos* is the over-activation of PARP1 following alkylating DNA damage or exposure to ROS[12,35]. Excessive activation of PARP1 leads to PAR accumulation, finally triggering AIMF1 release from mitochondria and AIFM1-mediated DNA fragmentation. PARP1 is also responsible for NAD+ and ATP depletion causing a fatal collapse in bioenergetics and redox metabolism (Supplemental Figure 3D).

Pyroptosis is triggered by innate immunity perturbations[36,37]. Variant cues, such as viral and bacterial products (LPS, is one of the major ones), trigger the formation of inflammasome followed by the activation of specific caspases including CASP1, CASP4 and CASP5. Such caspases cleave substrates such as GSDMD leading to pyroptosis. Moreover, pro-inflammatory interleukins IL1Beta and IL18 are also often secreted (Supplemental Figure 3E).

Ferroptosis relies on derailed redox regulation[38,39]. When antioxidant enzymes, mainly GPX4, are overwhelmed, membrane lipids are oxidized to peroxides, causing fatal alterations in membrane permeability, calcium waves, changes in membrane potential and cell death (Supplemental Figure 3F).

Interplay between modes of cell death and switch points

From the detailed RCD network, it is possible to deduce a scheme of the major players and interplay among them (Supplemental Table 1, Figure 3). The inputs at the top of the initiation layer dictate the choice of the pathway. However, the regulation of the chosen pathway is not trivial, because the same regulator can influence different cell death modes, depending on the presence of activators and inhibitors. It is also important to note that formation of high molecular weight complexes is essential step for initiation of all modes of cell death. Moreover, cooperation between cell death modes can occur. Once the choice of the cell death mode is made, the signalling propagates to the execution layer, resulting in different forms of cell death (outputs), each of which has a particular phenotype (Figure 3).

Engagement between the ligands and death receptors results in the initiation of signalling, as for example after interaction of TNF with its receptor, RIPK1 and CFLAR are recruited to the death receptor signalling complex (DISC) thanks to TRADD along with CASP8. Three major pathways emerge, depending on the recruited players and the degree of CASP8 oligomerization: apoptosis, necroptosis and pro-survival signalling. CFLAR prevents apoptosis triggering. In this situation, recruited RIPK1 is activated through polyubiquitination. Polyubiquitinated RIPK1 then activates IKK and MAP3K7 leading to the activation of the pro-survival transcription factor NF-κB. Moreover, RIPK1 phosphorylation by IKK and MAP3K7 prevents its interaction with FADD and CASP8 thus favouring RIPK1-independent apoptosis[40]. Members of the inhibitor of apoptosis protein family (IAP) also play an important role in these interactions. For example, one IAP called XIAP constitutively inhibits caspases in the physiological state. Other IAPS like BIRC2 and BIRC3 lead to an upregulation of anti-apoptotic factors and also ubiquitinate RIPK1, thus, triggering pro-survival NF-κB signalling[41,42]. However, some IAPs provoke CYLD dependent RIPK1 de-ubiquitination, that results in RIPK1 release from the necrosome complex, which drives extrinsic apoptosis[43].
Apoptosis strongly depends on energy supply, therefore in the absence of ATP, cells tend to undergo necrotic rather than apoptotic death. In specific circumstances, when AMPK is activated, BECN1 may favour CASP8 cleavage and apoptosis activation. Interestingly, both apoptotic and necroptotic machineries can be co-activated, if a combination of stimuli is applied on the cell or when apoptotic signalling is activated while mitochondria become permeabilized and releases factors that favour necroptosis, such as CYPD[45]. Autophagy normally maintains the energy status in the cell [34,44], however prolonged autophagy may result in cellular demise[46].

Reactive oxidative species (ROS) are widely implicated in most RCD modes. As they can act both as initiator and executor, depending on the RCD subroutine, ROS tend to increase interactions between cell death pathways. ROS accumulation favours BAX/BAK recruitment to mitochondria and thus acts as a major initiator of intrinsic apoptosis. ROS is also essential for successful release of Cytochrome C (CYCS) from mitochondria. In the same way, parthanatos can be a consequence of prolonged oxidative stress. Although the precise mechanism remains unknown, caspase activation has also been shown to generate ROS via the mitochondrial electron-transport chain[47]. Likewise, ferroptosis is based on the generation of an excessive amount of ROS.

Access and navigation of RCD map

The RCD map can be browsed online at https://navicell.curie.fr/pages/maps_rcd.html. The map is presented in three independent platforms, namely NaviCell, MINERVA[25] and NDEx[26] that can be accessed from the map home page. The map components are clickable, making it interactive. The extended annotations of the map components contain a rich tagging system converted to links. This allows tracing the involvement of molecules into different map sub-structures as meta-modules and modules. The tagging system also allows to use the map as a source of annotated signatures of different cell death modes (Figure 2 and Supplemental Figure 2).

The semantic zooming feature of NaviCell[62] simplifies navigation throughout the large collection of molecular interactions, revealing a readable amount of details at each zoom level. A gradual exclusion of details allows the exploration of map contents, going from the detailed towards the top-level view. The hierarchical structure of the RCD map as described above facilitated the generation of several zoom levels for web-based navigation of the map (Figure 2).

Comparison of RCD map with similar pathway resources

The map has been compared to the relevant pathways describing cell death-related processes from the KEGG[14] and REACTOME[15] pathway databases. Altogether these relevant selected pathways cover 956 HUGO names in KEGG and 805 HUGO names in REACTOME. These lists were compared with the RCD map that contains 891 HUGO names (Supplemental Table 2). This number is different than the one reported in Table 1 as we choose to only select HGNC approved gene symbol to have a reliable comparison with the two other databases. For example, "cleaved caspase1*" and "caspase 1*" count as two different entities in Table 1 but correspond to only one HGNC approved symbol (CASP1) in Supplemental Table 2.

Some RCD modules represent the processes at more detailed level in terms of the number of gene names, comparing to the corresponding pathways from KEGG and REACTOME databases. For example, Programmed Cell Death pathway in REACTOME contains 178 HUGO names, this corresponds to the Apoptosis and Necroptosis modules in RCD map, together covering 284 HUGO names. On the contrary, the necroptosis module is slightly more enriched in the KEGG pathway than in the RCD map (165 in KEGG vs. 154 in ACSN). However, in KEGG, the parthanatos pathway (especially the groups of histone genes) is included within the necroptosis module. In contrary, in the RCD map, parthanatos is described as an independent module and is updated with the most recent publications related to cancer. Some metabolic pathways are more represented in other databases, comparing to the RCD map, as this applies to the pentose phosphate pathway and porphyrin metabolism (that actually includes chlorophyll metabolism) in KEGG, as well as to fatty acid metabolism in REACTOME (Supplemental table 2). However, it is important to stress that metabolic reactions are not within the scope of the RCD map unless they modulate cell death-related processes.

The overlap of the RCD map HUGO names with other pathways reaches 47% for KEGG and 36% for REACTOME. 323 out of 805 HUGO names from REACTOME pathways and 423 out of 956 proteins from KEGG pathway are also present in RCD map (Figure 4A and Supplemental Table 2).

Remarkably, 375 HUGO names are unique for the RCD map (Figure 4A and Supplemental Figure 4A). These unique entities are homogeneously distributed across the map. More recently described RCD modes, such as ferroptosis and pyroptosis that are carefully represented in the RCD map are close-to-completely absent from KEGG and REACTOME. Altogether, we conclude that the contents of the RCD map are not redundant with other pathway databases and that a significant proportion of entities are unique to the RCD map.

We also compared the publications used to annotate the RCD map and the corresponding selected pathways in KEGG and REACTOME resources. Of note, 815 papers out of 829 papers that were used to annotate the RCD map are unique and are not referenced in the annotations of selected pathways from KEGG or Reactome (Supplemental Figure 4B). Although the median age of the literature references in the RCD map is older than in the corresponding pathways from the other two databases, 25% of the papers referenced in the RCD map have been published relatively recently, between 2010-2018 (Figure 4B).

Finally, the journal types represented in the three databases were compared. The range of the journals used for annotation of the RCD map and the other two databases is relatively similar. However, the distribution of the papers from different types of journals is rather different. In the annotations of the RCD map, the citations to journals in the area of molecular biology are overrepresented, compared to the other two databases. This indicates that the RCD map dwells into the molecular mechanisms rather than the phenotypic description of the process (Figure 4 C and D).

Taken together, the results of database comparisons indicate that the RCD resource is topic-specific, and covers all known modes of cell death mechanisms and their interplay. The thoughtful layout and visual organization of the biological knowledge displayed in the map makes it an attractive resource for data analysis.

Application of the RCD map to neurodegenerative and malignant diseases

Alzheimer's disease (AD) is a the most prevalent neurodegenerative disease in which neurons progressively succumb[63]. Nevertheless, the precise molecular processes resulting in neuronal cell death are elusive. To explore the RCD mechanisms involved in AD, gene expression data from three different studies was analysed (see STAR Methods), focusing on the Hippocampus, which is the most affected brain area in this disease[64]. In addition, the transcriptome of three non-small cell lung cancer (NSCLC) cohorts was studied, knowing that cancer is a disease characterized by the unwarranted survival of tumour cells.

The pathway scoring method ROMA was applied to quantify the module activity scores for both diseases using the module definition from RCD map as detailed in Martignetti *et al*.[65]. The module activity values were plotted on the RCD map using the BiNoM plugin of Cytoscape to visualize the differences between the two diseases[66].

The ROMA scores of AD and NSCLC exhibited rather inverse trend (Figure 5 and Supplemental Figures 5 and 6). Regarding RCD types, the modules corresponding to the TRAIL response, Pyroptosis and Dependence Receptors were more active in AD (Figure 5A). In contrast, in NSCLC, the ligand receptor modules (TNF response, TRAIL response and FAS response), as well as some modules of the signalling layer (Pyroptosis and Dependence Receptors), are less active (Figure 5A, Supplemental Figure 6).

Of note, most modules corresponding to the pyroptosis module appeared to be more active in Alzheimer disease. In addition, in NSCLC several metabolism-related modules (including glucose metabolism, oxidative

phosphorylation and the citrate cycle), as well as ER stress, were more active (Figure 5B and 5C). This metabolism-related modules activity confirm previous studies[67,68], including on the difference between Alzheimer's disease and lung cancer[69]. Indeed, the integrated comparison of the RCD map across AD and NSCLC is in line with speculations on the inverse comorbidity between both diseases[69–71], as well epidemiological studies suggesting that NSCLC occurs less frequently in AD patients than in age-matched individual without AD[72].

In the next step, the top contributing genes for each disease were identified. For this, the correlation coefficients in all the studies were calculated and those genes that had a correlation coefficient of minimum 0.5 (absolute value), with a significant p-value and appeared in at least 2 of the 3 data sets were selected (Supplemental Table 3). As a result, a list of genes that contribute either positively or negatively to each module, was retrieved.

In the case of Alzheimer, pyroptosis has been suggested and reviewed as a CASP1-dependent response to chronic aseptic inflammation[37,73]. Experimental evidence has linked pyroptosis in Alzheimer to the NLRP1 inflammasome[74] or NLRP3 inflammasome[75]. However, most studies correlating Alzheimer and pyroptosis have been performed in rodent models. Here, we identified *IL18*, *CASP4*, *GBP2*, *CASP1*, and *AIM2* as the genes that were contributing most to the pyroptosis module. *IL18* gene has been found to be over-expressed in brains of AD patients[76]. *CASP4* expression has been hypothesized to mediate inflammatory responses in AD pathology[77]. *CASP1*, together with other genes encoding caspases, has been found to be overexpressed in AD patients[78]. *AIM2* has been found in mouse models to promote IL1B secretion by neurons, which might also participate to AD pathology[79]. However, *GBP2* expression has not yet been evaluated for its potential role in AD pathology. Recently, Saresella and colleagues found that inflammasome components (NLRP1, NLRP3, PYCARD, CASP1, CASP5 and CASP8) and downstream effectors (IL1B, IL18) were upregulated in peripheral blood mononuclear cells from patients with moderate and severe AD[79]. All these findings support our results using the RCD map; nevertheless, future research is needed to elucidate if neuroinflammation leads to pyroptosis during AD pathology.

In cancer, ER stress has been identified as an adaptive response that favours either growth or apoptosis[80,81]. In addition, ER stress has also been related to chemotherapy resistance[82]. In our study, we identified the genes *PDIA6*, *PDIA4*, *DNAJB11*, *SEC61G*, *SEC61A1* and *CREB3L4* as positively contributing genes and *ITPR1*, *RYR2*, *NFKB1* and *NLRC4*, as negatively contributing genes for the ER stress module. *PDIA6* and *PDIA4* have been demonstrated to be overexpressed in NSCLC biopsies resistant to chemotherapy with cisplatin, and their silencing actually may reverse drug resistance[83]. The *NFKB1* gene has been described to be a key player in the ER stress pathway and in cancer survival mechanisms[84,85]. *NLRC4* is downregulated in lung cancer cases[86]. *NLRC4* contains a caspase recruitment domain (CARD) through which it can regulate apoptosis via NF-κB signalling pathways[86], suggesting a possible link between *NLRC4* and *NFKB1* genes in this module. In contrast, there are no consistent reports on the possible involvement of *DNAJB11*, *SEC61G*, *SEC61A*, and *CREB3L4* in NSCLC.

RCD signatures in different ovarian cancer subtypes

Ovarian cancer, the second most prevalent of the female genital tract, with a high mortality rate[87,88] (https://seer.cancer.gov/statfacts/html/ovary.html), encompasses a heterogeneous group of tumors, because different genetic, morphological and pathological characteristics are involved in the disease initiation and progression[87,88]. We analysed transcriptomics and copy number data from a cohort of 489 high-grade serous ovarian cancer accessible via the Cancer Genome Atlas (TCGA)[89,90]. Using a non-negative matrix factorization approach, these tumours have been clustered into four subtypes, namely: differentiated, immuno-reactive, mesenchymal, and proliferative, as reported elswhere[90].

Relying on these subtypes definitions, we applied ROMA analysis (see above) to mRNA expression data to this data set, while comparing the four ovarian cancer subtypes. The visualization of the ROMA scores in the context of RCD map revealed important differences among these subcategories (Figure 6). The differentiated subtype exhibited several active modules in the area of metabolism (mitochondrial metabolism, glucose metabolism, oxidative phosphorylation and TCA cycle). In contrast, apoptosis-related and starvation/autophagy-related modules appeared to be deactivated (Figure 6A). As to be expected[91], the immunoreactive subtype was characterized by the upregulation of the majority of the modules related to death receptor pathways and caspase-related executors (Figure 6B). In addition, we observed the activation of the modules initiated by inflammation, such as pyroptosis and – to a lower degree - starvation/autophagy (Figure 6C). The mesenchymal type, being the most aggressive one, displayed a high activity in some death-executing modules, with a notable suppression of oxidative phosphorylation and TCA cycle as well as the antioxidant response (Figure 6B). The proliferative subtype exhibited higher activity of the modules related to fatty acid biosynthesis, glutamine metabolism, and nuclear integrity (including the DNA damage response), all in line with the high replicative activity of this cancer subtype. In contrast, the majority of functional modules responsible for regulation and execution of cell death were strongly downregulated in the proliferative subtype (Figure 6E).

Visualising the copy number (CN) data of the different subtypes of ovarian cancer in the context of RCD map allowed us to see that the proliferative type corresponds to a higher number of CN gains, indicating massive genomic aberrations, compared to other subtypes (Figure 6), that represents an important negative prognostic factor [92,93]. For example, it is now known that *YWHAZ* promotes ovarian cancer metastasis by modulating glycolysis[94]. CN variations in *WISP1* have been associated with endometrial adenocarcinoma[95] whereas *NDRG1* has been reported as tumour suppressor in ovarian carcinogenesis across distinct ovarian subtypes[96,97] (Supplemental table 3), therefore it is thus not surprising to find these genes as top hits across ovarian cancer subtypes.

In synthesis, data visualization via RCD maps may constitute a useful tool for determining functionally relevant differences among cancer subtypes and between human disorders.

Discussion

Different RCD modes influence each other by their response to common inputs and a complex interplay between the molecules involved in their signalling and modulation. There is often a combination of cues, such as cellular energy status, external signals, as well as responses to DNA damage, that, in combination, can lead either to cell survival or to cell death through different scenarios. The existing linear and disconnected representations of regulated cell death mechanisms is far from satisfactory. In this work, we attempted to gather all available information about RCD mechanisms and to represent them in a structured and computer-readable manner. The comprehensive RCD map covers the initiating phases, the signalling phase during which the mode of the cell death is chosen, as well as the final and fatal execution phase.

Understanding the interplay between RCD modes represented in the form of comprehensive signalling map can help to evaluate the status of cell death modes in human diseases. This may be critical for choosing the correct treatment strategy and predicting therapeutic responses. For example, restoring caspase activity in cancer treatment by selective induction of apoptosis is one of the common goals of antineoplastic treatments, though hampered by the activation of apoptosis-inhibitory pathways. For this reason, it has been suggested to develop alternative agents that would activated alternative routes of RCD. As a speculative scenario, the induction of necroptosis, ferroptosis or autophagy-dependent death might offer an opportunity to kill cancer cells and – at least - to restore their sensitivity to cytotoxic drugs [11,16,33,34]. The RCD map will help to select the alternative routes by performing pathway analyses for each particular case.

The RCD map was designed to be part of ACSN resource as a tool for cancer research. Beyond this possibility, we demonstrate here that this resource can be applied to other pathologies. As aberrations in cell death control are involved in numerous diseases, the RDC map might be taken advantage of to explore pathologies including infectious diseases and degenerative processes. We demonstrated in this work that the RDC map is useful for the comparison of AD, a state of excessive cell death, and NSCLC, a pathology linked to the suppression of cell death pathways.

In summary, we anticipate that the RCD map will become useful for bioinformaticians and translational scientists interested in exploring aberrations in cell death pathways across distinct human pathologies.

STAR methods

Map availability

The RCD map is freely available at the web page https://navicell.curie.fr/pages/maps_rcd.html. The map is provided in three platforms, NaviCell, MINERVA and integrated into the repository NDEx. The RCD map can

be downloaded in several exchange formats. In addition, the content of RCD map grouped per modules is available and downloadable in the form of GMT files suitable for further functional data analysis.

Map construction

The signalling network of RCD regulation was manually constructed and based on information extracted from literature curation retrieved from the PubMed database. The map was composed using the CellDesigner tool[35] and the standard visual syntax Systems Biology Graphical Notation (SBGN)[36] for representing molecular biology mechanisms. The software creates a structured representation in Systems Biology Markup Language (SBML), suitable for further computational analysis[37]. Each entity of the map is annotated by corresponding references and specific notes.

Data model

The RCD map was constructed using a methodology previously described[27,98]. The maps are drawn using Process Description (PD) language of Systems Biology Graphical Notation (SBGN) syntax. The CellDesigner format represents a proprietary extension of the Systems Biology Markup Language (SBML)[28]. The most basic unit of RCD map is a biochemical reaction, formed by reactants, products and various types of regulators (Figure 1 and Supplemental Figure 1). The data model includes the following molecular objects: proteins, genes, RNAs, antisense RNAs, simple molecules, ions, drugs, phenotypes, complexes. These objects can play a role of reactants, products and regulators in a connected reaction network. The objects 'phenotypes' play a role of biological process outcome or readout. Edges on the maps represent biochemical reactions or reaction regulations of various types. Different reaction types represent posttranslational modifications, translation, transcription, complex formation or dissociation, transport, degradation and so on. Reaction regulations include catalysis, inhibition, modulation, trigger and physical stimulation. The naming system of the maps is based on HGNC-approved gene symbol, named as 'HUGO identifiers' in the text, for genes, proteins, RNAs and antisense RNAs and CAS/ChEBI identifiers for drugs, small molecules and ions. In addition, in some cases individual or generic entities are named by commonly used synonyms. In this case, the name is followed by an asterisk (e.g. 'p53*' instead of 'TP53'). In all cases, the HUGO identifier is provided in the protein notes. Subcellular localization of molecular entities is an important factor for the functioning and activity of the signalling processes. Cellular compartments such as cytoplasm, nucleus, mitochondria, etc. recapitulate the cellular architecture on the map (Supplemental Figure 1).

Literature selection rules

The rules for literature selection are as following: first five to ten reviews articles in the field were chosen for extracting the consensus pathways and regulations accepted in the field and for approaching to the literature suggested in these reviews. This allowed to construct the 'backbone' of the network and to define the biological processes boundaries (Figure 1). Further, information from original papers, preferably most recent studies, is analysed and added to enlarge and enrich the network. The decision about adding a biochemical event or

regulation or a process to the map has to be supported by at least two independent studies performed in different teams.

Map annotation format

Each entity and reaction on the map is annotated using the NaviCell annotation format (Supplemental Figure 2). The annotation includes three sections namely 'Identifiers', 'Maps_Modules' and 'References'. 'Identifiers' section provides links to the corresponding entity descriptions in HGNC, UniProt, Entrez, GeneCards, REACTOME, KEGG, and Wikipedia databases. 'Maps_Modules' section includes links to modules where the entity is found. 'References' section includes notes added by the map manager and links to relevant publications in PubMed. Annotations can be associated with a molecular entity (such as protein) as well as to its particular modification (such as a particular post-translational modification). NaviCell (described below) provides mechanisms of cross-referencing RCD map with other molecular and pathway databases, such as KEGG PATHWAY, Reactome, Atlas of Genetics and Cytogenetics in Oncology and Haematology, GeneCards, Wiki Genes and others.

Module tagging

A systematic tagging system was applied for annotation of each entity with module tags. The tags are converted into the links by the NaviCell factory in the process of online map version generation. The links allow to trace participation of entities in different modules of the map and also facilitate shuttling between these structures.

Generation of NaviCell map with NaviCell factory

CellDesigner map annotated in the NaviCell format is converted into the NaviCell web-based front-end, which is a set of html pages with integrated JavaScript code that can be launched in a web browser for online use. HUGO identifiers in the annotation form allow using NaviCell tool for visualization of omics data. A detailed guide of using the NaviCell factory embedded in the BiNoM Cytoscape plugin[66] is provided at https://navicell.curie.fr/doc/NaviCellMapperAdminGuide.pdf.

Map navigation

The content of RCD map is provided in the form of an interactive global map. The visualization and exploration of the RCD map are empowered by the NaviCell web-based environment (https://navicell.curie.fr). NaviCell uses Google Maps engine and principles for navigating through the content of the map. Thus, the logic of navigation as scrolling, zooming and features as markers, callout windows and zoom bar are adopted from the Google Maps interface. Map queries can be done using the search window or by selecting the entities of interest in the selection panel. The development of semantic zooming in NaviCell simplifies navigation through large maps of molecular interactions by providing several levels of map view. To facilitate the exploration, each level of zoom on the map exposes a certain depth of detail. In addition, navigation is also simplified by the modular

structure of the map where each module map can be visualized individually. Shuttling between the global map to modular maps usng the map icon (globe) (Figure 2 and Supplemental Figure 2).

Web-based platforms support

The RCD map is available at other platforms such as MINERVA[25] and NDEx[26]. To integrate maps within NDEx, CellDesigner map was first loaded to Cytoscape using the BiNoM Cytoscape plugin and then uploaded on NDEx using the CyNDEx Cytoscape plugin.

Map structural analysis

The map backbone structure was manually built based on selection of major inputs and output in each functional module of the map (Supplemental table 1). For each module, major inputs and outputs were selected on the map by tags from the RCD map, extracted and further manually refined based on number of interactions and reviews of the literature. The backbone structure of the network was restored using the information from the comprehensive RCD map. Each cell death mode was first represented as a separate diagram (Supplemental Figure 3). All diagrams were gathered together to create the global scheme, where interplays between different cell death modes were included (Figure 3).

Data Acquisition

Gene expression datasets from lung cancer and Alzheimer's disease (GSE36980, GSE48350, GSE5281, GSE19188, GSE19804, GSE33532) were downloaded from the Gene Expression Omnibus (GEO, https://www.ncbi.nlm.nih.gov/geo/). For the testing, we grouped the cases of each disease and compared them to their respective controls. The ovarian cancer data was obtained from The Cancer Genome Atlas (TCGA)[89,92]. The group definitions for the ovarian cancer cases were used as previously described by using a non-negative matrix factorization approach[92].

Module scores calculation and visualization

The Representation of Module Activity (ROMA) analysis[65] was performed, using the "rRoma" and "rRomaDash" R packages (available at : https://github.com/sysbio-curie/rRoma and https://github.com/sysbio-curie/rRomaDash). ROMA quantifies the statistical significance of the variance explained by the first principal component (overdispersion) computed for an expression matrix limited to the genes in the module, and attributes a score for each pathway in each sample. With the analysis provided by ROMA, we identified the over-dispersed modules in RCD map. Further, one tailed pairwise *t*-tests using the ROMA scores from all modules was done, to determine module activity directionality. Then the calculation of the top contributing genes was performed per module using Pearson's correlation, selecting those with an absolute correlation coefficient of 0.5 minimum. Significance level was considered when $p < 0.01$. Colored map images were obtained using function "Stain CellDesigner map" from BiNoM Cytoscape plugin[99] using xml map files and the

average relative ROMA scores from the analysis described above. In addition, Gene Set Enrichment Analysis (GSEA)[100] was also performed to corroborate the results in the ROMA Analysis (data not shown).

Acknowledgments

We thank Mathurin Dorel for help with data analysis in the context of the map and Maria Kondratova for layout and modular structure design. This work has been funded by INSERM Plan Cancer N° BIO2014-08 COMET grant under ITMO Cancer BioSys program. This work received support from MASTODON program by CNRS (project APLIGOOGLE) and COLOSYS grant ANR-15-CMED-0001-04, provided by the Agence Nationale de la Recherche under the frame of ERACoSysMed-1, the ERA-Net for Systems Medicine in clinical research and medical practice. GK and EB were sponsored by the HTE Inserm/ITMO Cancer program. GK is supported by the Ligue contre le Cancer (équipe labellisée); Agence National de la Recherche (ANR) – Projets blancs; ANR under the frame of E-Rare-2, the ERA-Net for Research on Rare Diseases; Association pour la recherche sur le cancer (ARC); Cancéropôle Ile-de-France; Chancelerie des universités de Paris (Legs Poix), Fondation pour la Recherche Médicale (FRM); a donation by Elior; European Research Area Network on Cardiovascular Diseases (ERA-CVD, MINOTAUR); Gustave Roussy Odyssea, the European Union Horizon 2020 Project Oncobiome; Fondation Carrefour; High-end Foreign Expert Program in China (GDW20171100085 and GDW20181100051), Institut National du Cancer (INCa); Institut Universitaire de France; LeDucq Foundation; the LabEx Immuno-Oncology; the RHU Torino Lumière; the Seerave Foundation; the SIRIC Stratified Oncology Cell DNA Repair and Tumor Immune Elimination (SOCRATE); and the SIRIC Cancer Research and Personalized Medicine (CARPEM).

Conflict of Interest

The authors declare no conflict of interest.

Abbreviations

RCD, programmed cell death; MOMP, Mitochondrial outer membrane permeabilization; ER: Endoplasmic reticulum

Figure legends

Figure 1. Regulated Cell Death map construction workflow. The scheme depicts the steps of map construction starting from collection of cancer-specific and RCD-related information about individual molecular interactions from scientific publications and databases, manual annotation and curation of this information, then organization of the formalized knowledge in form of global map with modular structure.

Figure 2. Regulated Cell Death map browsing, zooms and entities annotations. (A) Map interface in NaviCell-powered Google Maps platform with a top view layout of RCD map. The interface includes the map window, selection panel, data analysis panel and upper panel. Map querying is possible via the search window or by checking on the entity in a list of entities in the selection panel that will drop markers all over the map (for example, Caspase 9). (B) Zoom of a fragment of the map and callout window. Clicking on a marker opens a callout window containing three sections: 'Identifiers' with links to external databases; 'Map Modules' with links to functional modules where the entity of interest is found, 'References' with links to PubMed, and annotation notes. Clicking on the 'globe' icon opens the corresponding map. Clicking on a 'book' icon opens a detailed annotation page. (C) Zoom of a fragment of a module showing the most detailed level of the representation of molecular mechanisms. The participation of the selected molecule (e.g. caspase 9) in various reactions and complexes can be seen.

Figure 3. Interplay among regulated cell death modes. Major players were selected on the RCD map by tags and the scheme was deduced from the map and further manually edited based on the number of interactions on the RCD maps and information from the literature. For simplification, the signalling is represented in the form of an activity flow diagram indicating either activation or inhibition. Some molecular entities are grouped into a generic entity representing either a molecular complex or a reaction cascade. HGNC nomenclature was used, except for entities marked by stars, for which common names were used. RCD modes are highlighted by the coloured semi-transparent background. Most of the pathways are drawn from the top (initiation) to the bottom of the figure (execution). Some incidences of cross-talk between pathways are clearly illustrated. ROS production is a crucial input and output of RCD. Death receptor can trigger a great variety of responses, even cell survival (via induction of IAP, NFKB1). Apoptosis, necroptosis and autophagy are interconnected processes (through multifunctional implications of CFLAR, PARP1, IAP, BECN1). Energy supply is a major regulator of cell fate. IAP: Inhibitors of apoptosis proteins (IAP); LPS: lipopolysaccharides; MAMPs: microbe-associated molecular patterns; PTPC: permeability transition complex; MPT: mitochondrial permeability transition; LC3: microtubule associated protein 1 light chain 3 beta (MAP1LC3B).

Figure 4. Comparison of RCD Map with other pathway resources. (A) Comparison of HUGO names content in selected pathways from REACTOME and KEGG databases with the RCD map. The Venn diagram shows the overlap of HUGO names between different databases. Distribution of (B) publication years and (C) journals annotating the selected pathways from the REACTOME, KEGG and RCD map. (D) Relative distribution of journals types used for annotation of the selected pathways from REACTOM, KEGG and RCD map.

Figure 5. Visualization of average ROMA modules activity scores using expression data from Alzheimer disease (AD) hippocampus samples and NSCLC specimens in the RCD map. (A) Heatmap representing ROMA scores for the two diseases (each respective to its normal controls). Staining of RCD map with ROMA scores from (B) AD data and (C) NSCLC data. The plotted values correspond to the relative ROMA module score compared to controls (as in A).

Figure 6. Visualization of expression and genomic data from ovarian cancer groups. (A) differentiated, (B) mesenchymal, (C) immunoreactive, (D) proliferative subtype. The background colour represents the expression value per protein (red: up-regulated, green: down-regulated). The glyphs (triangles) represent increased gene copy number, 4 copies and up. (E) Heat map of the ROMA scores per subtype.

Tables

Table 1. Structure and content of RCD signalling network map

Supplemental information

Supplemental text: Description of the RCD content. Functional meta-modules and modules of the map

Supplemental Table 1. List of key input and output players in RCD map modules

Supplemental Table 2. Comparison of gene content between pathways from KEGG and REACTOME databases to the Regulated Cell Death map. HUGO names were used as common IDs.

Supplemental Figure 1. Data model

Supplemental Figure 2. Annotation page on an entity on RCD map using NaviCell format.

Supplemental Figure 3. Representation of regulated cell death modes in a form of activity flow diagrams including inputs (in green), key players and outputs (in red). (A) Apoptosis, (B) Necroptosis, (C) Autophagy- and lysosome-dependent cell death, (D) Parthanatos, (E) Pyroptosis, (F) Ferroptosis, (G) Mitochondrial permeability transition-driven necrosis.

Supplemental Figure 4. Comparison of the Regulated Cell Death Map with other pathway resources. (A) Visualization of unique genes distribution from the RCD map across functional modules. (B) Venn diagram shows intersection of the publications annotating the selected pathways from the sources.

Supplemental Figure 5. Boxplots corresponding to the ROMA scores in different modules across the six studies for the comparisons of Alzheimer's disease and lung cancer.

Supplemental Figure 6. Heatmap representing ROMA scores averaged between the three studies, separating disease groups and controls.

Supplemental Table 3. Top contributing genes per module for Alzheimer and lung cancer datasets. Green: positively contributing genes, red: negatively contributing genes.

References

1. Kang K, Lee S-R, Piao X, Hur GM. Post-translational modification of the death receptor complex as a potential therapeutic target in cancer. *Arch Pharm Res*. 2019;42(1):76-87. doi:10.1007/s12272-018-01107-8
2. Pentimalli F, Grelli S, Di Daniele N, Melino G, Amelio I. Cell death pathologies: targeting

death pathways and the immune system for cancer therapy. *Genes Immun*. December 2018. doi:10.1038/s41435-018-0052-x

3. Ouyang L, Shi Z, Zhao S, et al. Programmed cell death pathways in cancer: a review of apoptosis, autophagy and programmed necrosis. *Cell Prolif*. 2012;45(6):487-498. doi:10.1111/j.1365-2184.2012.00845.x
4. Stevens JB, Abdallah BY, Liu G, et al. Heterogeneity of cell death. *Cytogenet Genome Res*. 2013;139(3):164-173. doi:000348679 [pii]10.1159/000348679
5. Kaczmarek A, Vandenabeele P, Krysko D V. Necroptosis: the release of damage-associated molecular patterns and its physiological relevance. *Immunity*. 2013;38(2):209-223. doi:S1074-7613(13)00058-7 [pii]10.1016/j.immuni.2013.02.003
6. Lalaoui N, Lindqvist LM, Sandow JJ, Ekert PG. The molecular relationships between apoptosis, autophagy and necroptosis. *Semin Cell Dev Biol*. 2015. doi:10.1016/j.semcdb.2015.02.003
7. Galluzzi L, Vitale I, Aaronson SA, et al. Molecular mechanisms of cell death: recommendations of the Nomenclature Committee on Cell Death 2018. *Cell Death Differ*. 2018;25(3):486-541. doi:10.1038/s41418-017-0012-4
8. Yatim N, Cullen S, Albert ML. Dying cells actively regulate adaptive immune responses. *Nat Rev Immunol*. 2017;17(4):262-275. doi:10.1038/nri.2017.9
9. Ellis RE, Yuan JY, Horvitz HR. Mechanisms and functions of cell death. *Annu Rev Cell Biol*. 1991;7:663-698. doi:10.1146/annurev.cb.07.110191.003311
10. Russell RC, Yuan H-X, Guan K-L. Autophagy regulation by nutrient signalling. *Cell Res*. 2014;24(1):42-57. doi:10.1038/cr.2013.166
11. Xie Y, Hou W, Song X, et al. Ferroptosis: process and function. *Cell Death Differ*. January 2016. doi:10.1038/cdd.2015.158
12. Fatokun AA, Dawson VL, Dawson TM. Parthanatos: Mitochondrial-linked mechanisms and therapeutic opportunities. *Br J Pharmacol*. 2014;171(8):2000-2016. doi:10.1111/bph.12416
13. Kanehisa M. The KEGG database. *Novartis Found Symp*. 2002;247:91-93,119-128,244-252. http://www.ncbi.nlm.nih.gov/entrez/query.fcgi?cmd=Retrieve&db=PubMed&dopt=Citation&list_uids=12539951.
14. Kanehisa M, Goto S, Sato Y, Furumichi M, Tanabe M. KEGG for integration and interpretation of large-scale molecular data sets. *Nucleic Acids Res*. 2012;40(D1):D109-D114. doi:10.1093/nar/gkr988
15. Croft D, Mundo AF, Haw R, et al. The Reactome pathway knowledgebase. *Nucleic Acids Res*. 2014;42(D1):D472-D477. doi:10.1093/nar/gkt1102
16. Hoffmann R. A wiki for the life sciences where authorship matters. *Nat Genet*. 2008;40(9):1047-1051. doi:ng.f.217 [pii]10.1038/ng.f.217
17. Perfetto L, Briganti L, Calderone A, et al. SIGNOR: a database of causal relationships between biological entities. *Nucleic Acids Res*. 2016;44(D1):D548-54.

doi:10.1093/nar/gkv1048

18. Calzone L, Gelay A, Zinovyev A, Radvanyi F, Barillot E. A comprehensive modular map of molecular interactions in RB/E2F pathway. *Mol Syst Biol*. 2008;4:173. doi:10.1038/msb.2008.7
19. Caron E, Ghosh S, Matsuoka Y, et al. A comprehensive map of the mTOR signalling network. *Mol Syst Biol*. 2010;6:453. doi:10.1038/msb.2010.108
20. Mizuno S, Iijima R, Ogishima S, et al. AlzPathway: a comprehensive map of signalling pathways of Alzheimer's disease. *BMC Syst Biol*. 2012;6:52. doi:1752-0509-6-52 [pii]10.1186/1752-0509-6-52
21. Matsuoka Y, Matsumae H, Katoh M, et al. A comprehensive map of the influenza A virus replication cycle. *BMC Syst Biol*. 2013;7:97. doi:1752-0509-7-97 [pii]10.1186/1752-0509-7-97
22. Kuperstein I, Bonnet E, Nguyen H-A, et al. Atlas of Cancer Signalling Network: a systems biology resource for integrative analysis of cancer data with Google Maps. *Oncogenesis*. 2015;4(7):e160-e160. doi:10.1038/oncsis.2015.19
23. Mazein A, Ostaszewski M, Kuperstein I, et al. Systems medicine disease maps: community-driven comprehensive representation of disease mechanisms. *NPJ Syst Biol Appl*. 2018;4(1):21. doi:10.1038/s41540-018-0059-y
24. Dorel M, Viara E, Barillot E, Zinovyev A, Kuperstein I. NaviCom: a web application to create interactive molecular network portraits using multi-level omics data. *Database*. 2017;2017(1). doi:10.1093/database/bax026
25. Gawron P, Ostaszewski M, Satagopam V, et al. MINERVA-a platform for visualization and curation of molecular interaction networks. *NPJ Syst Biol Appl*. 2016;2(1):16020. doi:10.1038/npjsba.2016.20
26. Pratt D, Chen J, Pillich R, et al. NDEx 2.0: A Clearinghouse for Research on Cancer Pathways. *Cancer Res*. 2017;77(21):e58-e61. doi:10.1158/0008-5472.CAN-17-0606
27. Kondratova M, Sompairac N, Barillot E, Zinovyev A, Kuperstein I. Signalling maps in cancer research: construction and data analysis. *Database*. 2018;2018. doi:10.1093/database/bay036
28. Le Novère N, Hucka M, Mi H, et al. The Systems Biology Graphical Notation. *Nat Biotechnol*. 2009;27(8):735-741. doi:10.1038/nbt0909-864d
29. Kitano H, Funahashi A, Matsuoka Y, Oda K. Using process diagrams for the graphical representation of biological networks. *Nat Biotechnol*. 2005;23(8):961-966. doi:nbt1111 [pii]10.1038/nbt1111
30. Ashkenazi A, Dixit VM. Death receptors: signalling and modulation. *Science*. 1998;281(5381):1305-1308. http://www.ncbi.nlm.nih.gov/pubmed/9721089. Accessed March 6, 2019.
31. Dickens LS, Powley IR, Hughes MA, MacFarlane M. The 'complexities' of life and death: Death receptor signalling platforms. *Exp Cell Res*. 2012;318(11):1269-1277.

doi:10.1016/j.yexcr.2012.04.005

32. Czabotar PE, Lessene G, Strasser A, Adams JM. Control of apoptosis by the BCL-2 protein family: implications for physiology and therapy. *Nat Rev Mol Cell Biol*. 2014;15(1):49-63. doi:10.1038/nrm3722
33. Vandenabeele P, Galluzzi L, Vanden Berghe T, Kroemer G. Molecular mechanisms of necroptosis: an ordered cellular explosion. *Nat Rev Mol Cell Biol*. 2010;11(10):700-714. doi:nrm2970 [pii] 10.1038/nrm2970
34. Galluzzi L, Kepp O, Trojel-Hansen C, Kroemer G. Mitochondrial control of cellular life, stress, and death. *Circ Res*. 2012;111(9):1198-1207. doi:10.1161/CIRCRESAHA.112.268946
35. David KK, Andrabi SA, Dawson TM, Dawson VL. Parthanatos, a messenger of death. *Front Biosci (Landmark Ed*. 2009;14:1116-1128. http://www.ncbi.nlm.nih.gov/pubmed/19273119. Accessed October 10, 2017.
36. Shi J, Gao W, Shao F. Pyroptosis: Gasdermin-Mediated Programmed Necrotic Cell Death. *Trends Biochem Sci*. 2017;42(4):245-254. doi:10.1016/j.tibs.2016.10.004
37. Mamik MK, Power C. Inflammasomes in neurological diseases: Emerging pathogenic and therapeutic concepts. *Brain*. 2017;140(9):2273-2285. doi:10.1093/brain/awx133
38. Magtanong L, Ko PJ, Dixon SJ. Emerging roles for lipids in non-apoptotic cell death. *Cell Death Differ*. 2016;23(7):1099-1109. doi:10.1038/cdd.2016.25
39. Latunde-Dada GO. Ferroptosis: Role of lipid peroxidation, iron and ferritinophagy. *Biochim Biophys Acta - Gen Subj*. 2017;1861(8):1893-1900. doi:10.1016/j.bbagen.2017.05.019
40. Geng J, Ito Y, Shi L, et al. Regulation of RIPK1 activation by TAK1-mediated phosphorylation dictates apoptosis and necroptosis. *Nat Commun*. 2017;8(1):359. doi:10.1038/s41467-017-00406-w
41. Silke J, Vucic D. *IAP Family of Cell Death and Signalling Regulators*. Vol 545. 1st ed. Elsevier Inc.; 2014. doi:10.1016/B978-0-12-801430-1.00002-0
42. Witt A, Vucic D. Diverse ubiquitin linkages regulate RIP kinases-mediated inflammatory and cell death signalling. *Cell Death Differ*. 2017;24(7):1160-1171. doi:10.1038/cdd.2017.33
43. Hitomi J, Christofferson DE, Ng A, et al. Identification of a Molecular Signalling Network that Regulates a Cellular Necrotic Cell Death Pathway. *Cell*. 2008;135(7):1311-1323. doi:10.1016/j.cell.2008.10.044
44. Chaabane W, User SD, El-Gazzah M, et al. Autophagy, apoptosis, mitoptosis and necrosis: interdependence between those pathways and effects on cancer. *Arch Immunol Ther Exp*. 2013;61(1):43-58. doi:10.1007/s00005-012-0205-y
45. Galluzzi L, Kepp O, Krautwald S, Kroemer G, Linkermann A. Molecular mechanisms of regulated necrosis. *Semin Cell Dev Biol*. 2014;35:24-32. doi:10.1016/j.semcdb.2014.02.006
46. Tsuchihashi NA, Hayashi K, Dan K, et al. Autophagy through 4EBP1 and AMPK regulates oxidative stress-induced premature senescence in auditory cells. *Oncotarget*. 2015;6(6):3644-3655. doi:2874 [pii]

47. Choi K, Ryu S-W, Song S, Choi H, Kang SW, Choi C. Caspase-dependent generation of reactive oxygen species in human astrocytoma cells contributes to resistance to TRAIL-mediated apoptosis. *Cell Death Differ*. 2010;17(5):833-845. doi:10.1038/cdd.2009.154
48. Bartel DP. MicroRNAs: target recognition and regulatory functions. *Cell*. 2009;136(2):215-233. doi:10.1016/j.cell.2009.01.002
49. Thomas MP, Lieberman J. Live or let die: posttranscriptional gene regulation in cell stress and cell death. *Immunol Rev*. 2013;253(1):237-252. doi:10.1111/imr.12052
50. Lima RT, Busacca S, Almeida GM, Gaudino G, Fennell DA, Vasconcelos MH. MicroRNA regulation of core apoptosis pathways in cancer. *Eur J Cancer*. 2011;47(2):163-174. doi:S0959-8049(10)01073-7 [pii]10.1016/j.ejca.2010.11.005
51. Bienertova-Vasku J, Sana J, Slaby O. The role of microRNAs in mitochondria in cancer. *Cancer Lett*. 2013;336(1):1-7. doi:10.1016/j.canlet.2013.05.001
52. Frankel LB, Lund AH. MicroRNA regulation of autophagy. *Carcinogenesis*. 2012;33(11):2018-2025. doi:bgs266 [pii] 10.1093/carcin/bgs266
53. Tufekci KU, Meuwissen RL, Genc S. The Role of MicroRNAs in Biological Processes. *Methods Mol Biol*. 2014;1107:15-31. doi:10.1007/978-1-62703-748-8_2
54. Farazi TA, Hoell JI, Morozov P, Tuschl T. MicroRNAs in human cancer. *Adv Exp Med Biol*. 2013;774:1-20. doi:10.1007/978-94-007-5590-1_1
55. Serpico D, Molino L, Di Cosimo S. microRNAs in breast cancer development and treatment. *Cancer Treat Rev*. 2013. doi:S0305-7372(13)00230-2 [pii]10.1016/j.ctrv.2013.11.002
56. Wang G, Wang W, Gao W, Lv J, Fang J. Two functional polymorphisms in microRNAs and lung cancer risk: a meta-analysis. *Tumor Biol*. 2013. doi:10.1007/s13277-013-1355-1
57. Czochor JR, Glazer PM. microRNAs in Cancer Cell Response to Ionizing Radiation. *Antioxid Redox Signal*. 2013. doi:10.1089/ars.2013.5718
58. Metheetrairut C, Slack FJ. MicroRNAs in the ionizing radiation response and in radiotherapy. *Curr Opin Genet Dev*. 2013;23(1):12-19. doi:S0959-437X(13)00010-5 [pii]10.1016/j.gde.2013.01.002
59. Hata A, Lieberman J. Dysregulation of microRNA biogenesis and gene silencing in cancer. 2015;8(368):1-12.
60. Lu J, Getz G, Miska EA, et al. MicroRNA expression profiles classify human cancers. *Nature*. 2005;435(7043):834-838. doi:10.1038/nature03702
61. Zhang C, Peng G. Non-coding RNAs: An emerging player in DNA damage response. *Mutat Res Mutat Res*. 2015;763:202-211. doi:10.1016/j.mrrev.2014.11.003
62. Kuperstein I, Cohen DP, Pook S, et al. NaviCell: a web-based environment for navigation, curation and maintenance of large molecular interaction maps. *BMC Syst Biol*. 2013;7(1):100. doi:10.1186/1752-0509-7-100
63. Sperling RA, Aisen PS, Beckett LA, et al. Toward defining the preclinical stages of Alzheimer's disease: Recommendations from the National Institute on Aging-Alzheimer's

Association workgroups on diagnostic guidelines for Alzheimer's disease. *Alzheimer's Dement*. 2011;7(3):280-292. doi:10.1016/j.jalz.2011.03.003

64. Raskin J, Cummings J, Hardy J, Schuh K, Dean RA. Neurobiology of Alzheimer's Disease: Integrated Molecular, Physiological, Anatomical, Biomarker, and Cognitive Dimensions. *Curr Alzheimer Res*. 2015;12:712-722. doi:1875-5828/1
65. Martignetti L, Calzone L, Bonnet E, Barillot E, Zinovyev A. ROMA: Representation and quantification of module activity from target expression data. *Front Genet*. 2016;7(FEB):1-12. doi:10.3389/fgene.2016.00018
66. Bonnet E, Calzone L, Rovera D, Stoll G, Barillot E, Zinovyev A. BiNoM 2.0, a Cytoscape plugin for accessing and analyzing pathways using standard systems biology formats. *BMC Syst Biol*. 2013;7(1):18. doi:10.1186/1752-0509-7-18
67. Competition L, Affects D, In I. NIH Public Access. 2008;86(12):3279-3288. doi:10.1007/s11103-011-9767-z.Plastid
68. Liang WS, Reiman EM, Valla J, et al. Alzheimer's disease is associated with reduced expression of energy metabolism genes in posterior cingulate neurons. *Proc Natl Acad Sci U S A*. 2008;105(11):4441-4446. doi:10.1073/pnas.0709259105
69. Sánchez-Valle J, Tejero H, Ibáñez K, et al. A molecular hypothesis to explain direct and inverse co-morbidities between Alzheimer's Disease, Glioblastoma and Lung cancer. *Sci Rep*. 2017. doi:10.1038/s41598-017-04400-6
70. Musicco M, Adorni F, Di Santo S, et al. Inverse occurrence of cancer and Alzheimer disease: A population-based incidence study. *Neurology*. 2013;81(4):322-328. doi:10.1212/WNL.0b013e31829c5ec1
71. Ou SM, Lee YJ, Hu YW, et al. Does Alzheimer's disease protect against cancers? A nationwide population-based study. *Neuroepidemiology*. 2012;40(1):42-49. doi:10.1159/000341411
72. Tabarés-Seisdedos R, Baudot A. Editorial: Direct and Inverse Comorbidities Between Complex Disorders. *Front Physiol*. 2016;7:117. doi:10.3389/fphys.2016.00117
73. Patel MN, Carroll RG, Galván-Peña S, et al. Inflammasome Priming in Sterile Inflammatory Disease. *Trends Mol Med*. 2017;23(2):165-180. doi:10.1016/j.molmed.2016.12.007
74. Kaushal V, Dye R, Pakavathkumar P, et al. Neuronal NLRP1 inflammasome activation of Caspase-1 coordinately regulates inflammatory interleukin-1-beta production and axonal degeneration-associated Caspase-6 activation. *Cell Death Differ*. 2015;22(10):1676-1686. doi:10.1038/cdd.2015.16
75. Schmid-Burgk JL, Chauhan D, Schmidt T, et al. A genome-wide CRISPR (clustered regularly interspaced short palindromic repeats) screen identifies NEK7 as an essential component of NLRP3 inflammasome activation. *J Biol Chem*. 2016;291(1):103-109. doi:10.1074/jbc.C115.700492
76. Ojala J, Alafuzoff I, Herukka SK, van Groen T, Tanila H, Pirttilä T. Expression of

interleukin-18 is increased in the brains of Alzheimer's disease patients. *Neurobiol Aging*. 2009;30(2):198-209. doi:10.1016/j.neurobiolaging.2007.06.006

77. Kajiwara Y, McKenzie A, Dorr N, et al. The human-specific CASP4 gene product contributes to Alzheimer-related synaptic and behavioural deficits. *Hum Mol Genet*. 2016;25(19):4315-4327. doi:10.1093/hmg/ddw265
78. PN P, Yemul S, Xiang Z, Al E. CAspase gene expression in the brain as a function of the clinical progression of alzheimer disease. *Arch Neurol*. 2003;60(3):369-376. http://dx.doi.org/10.1001/archneur.60.3.369.
79. Saresella M, La Rosa F, Piancone F, et al. The NLRP3 and NLRP1 inflammasomes are activated in Alzheimer's disease. *Mol Neurodegener*. 2016;11(1):1-14. doi:10.1186/s13024-016-0088-1
80. Giampietri C, Petrungaro S, Conti S, Facchiano A, Filippini A, Ziparo E. Cancer microenvironment and endoplasmic reticulum stress response. *Mediators Inflamm*. 2015;2015. doi:10.1155/2015/417281
81. Avril T, Vauléon E, Chevet E. Endoplasmic reticulum stress signalling and chemotherapy resistance in solid cancers. *Oncogenesis*. 2017;6(8):e373. doi:10.1038/oncsis.2017.72
82. Salaroglio IC, Panada E, Moiso E, et al. PERK induces resistance to cell death elicited by endoplasmic reticulum stress and chemotherapy. *Mol Cancer*. 2017;16(1):1-13. doi:10.1186/s12943-017-0657-0
83. Tufo G, Jones AWE, Wang Z, et al. The protein disulfide isomerases PDIA4 and PDIA6 mediate resistance to cisplatin-induced cell death in lung adenocarcinoma. *Cell Death Differ*. 2014;21(5):685-695. doi:10.1038/cdd.2013.193
84. Xia Y, Shen S, Verma IM. NF- B, an Active Player in Human Cancers. *Cancer Immunol Res*. 2014;2(9):823-830. doi:10.1158/2326-6066.CIR-14-0112
85. Logue SE, Cleary P, Saveljeva S, Samali A. New directions in ER stress-induced cell death. *Apoptosis*. 2013;18(5):537-546. doi:10.1007/s10495-013-0818-6
86. Välk K, Vooder T, Kolde R, et al. Gene expression profiles of non-small cell lung cancer: survival prediction and new biomarkers. *Oncology*. 2010;79(3-4):283-292. doi:10.1159/000322116
87. McCluggage WG. Morphological subtypes of ovarian carcinoma: a review with emphasis on new developments and pathogenesis. *Pathology*. 2011;43(5):420-432. doi:10.1097/PAT.0b013e328348a6e7
88. Gilks CB, Prat J. Ovarian carcinoma pathology and genetics: recent advances. *Hum Pathol*. 2009;40(9):1213-1223. doi:10.1016/j.humpath.2009.04.017
89. Tomczak K, Czerwińska P, Wiznerowicz M. The Cancer Genome Atlas (TCGA): an immeasurable source of knowledge. *Contemp Oncol (Poznan, Poland)*. 2015;19(1A):A68-77. doi:10.5114/wo.2014.47136
90. Bell D, Berchuck A, Birrer M, et al. Integrated genomic analyses of ovarian carcinoma.

Nature. 2011;474(7353):609-615. doi:10.1038/nature10166

91. Konecny GE, Wang C, Hamidi H, et al. Prognostic and Therapeutic Relevance of Molecular Subtypes in High-Grade Serous Ovarian Cancer. *JNCI J Natl Cancer Inst*. 2014;106(10). doi:10.1093/jnci/dju249
92. Bell D, Berchuck A, Birrer M, et al. Integrated genomic analyses of ovarian carcinoma. *Nature*. 2011;474(7353):609-615. doi:10.1038/nature10166
93. Etemadmoghadam D, deFazio A, Beroukhim R, et al. Integrated Genome-Wide DNA Copy Number and Expression Analysis Identifies Distinct Mechanisms of Primary Chemoresistance in Ovarian Carcinomas. *Clin Cancer Res*. 2009;15(4):1417-1427. doi:10.1158/1078-0432.CCR-08-1564
94. Shi J, Ye J, Fei H, et al. YWHAZ promotes ovarian cancer metastasis by modulating glycolysis. *Oncol Rep*. 2018;41(2):1101-1112. doi:10.3892/or.2018.6920
95. Tang Q, Jiang X, Li H, et al. Expression and prognostic value of WISP-1 in patients with endometrial endometrioid adenocarcinoma. *J Obstet Gynaecol Res*. 2011;37(6):606-612. doi:10.1111/j.1447-0756.2011.01631.x
96. WANG B, LI J, YE Z, LI Z, WU X. N-myc downstream regulated gene 1 acts as a tumor suppressor in ovarian cancer. *Oncol Rep*. 2014;31(5):2279-2285. doi:10.3892/or.2014.3072
97. Zhang D, Chen P, Zheng C-H, Xia J. Identification of ovarian cancer subtype-specific network modules and candidate drivers through an integrative genomics approach. *Oncotarget*. 2016;7(4):4298-4309. doi:10.18632/oncotarget.6774
98. Kuperstein I, Bonnet E, Nguyen H-A, et al. Atlas of Cancer Signalling Network: a systems biology resource for integrative analysis of cancer data with Google Maps. *Oncogenesis*. 2015;4(7):e160-e160. doi:10.1038/oncsis.2015.19
99. Zinovyev A, Viara E, Calzone L, Barillot E. BiNoM: A Cytoscape plugin for manipulating and analyzing biological networks. *Bioinformatics*. 2008;24(6):876-877. doi:10.1093/bioinformatics/btm553
100. Subramanian A, Tamayo P, Mootha VK, et al. Gene set enrichment analysis: a knowledge-based approach for interpreting genome-wide expression profiles. *Proc Natl Acad Sci U S A*. 2005;102(43):15545-15550. doi:10.1073/pnas.0506580102

Table 1: Structure and content of RCD map

Layer/Module	Chemical Species (Entities)	Proteins	Genes	RNAs	asRNAs	Reactions
Initiation (reversible)						
STRESS RESPONSE						
ANTIOXIDANT RESPONSE	213	151	4	9	12	95
DNA DAMAGE RESPONSE	128	59	3	3	5	80
ER STRESS	382	161	45	44	4	291
STARVATION-AUTOPHAGY	438	165	19	31	31	290
LIGAND RECEPTOR						
DEATH RECEPTOR PATHWAYS	640	287	23	27	32	469
TRAIL RESPONSE	36	25	0	0	0	18
FAS RESPONSE	29	24	0	0	0	14
TNF RESPONSE	87	39	3	3	0	57
DEPENDENCE RECEPTORS	78	52	0	0	0	36
METABOLISM						
CELL METABOLISM						
FATTY ACID BIOSYNTHESIS	78	34	1	3	2	33
GLUCOSE METABOLISM	190	112	0	0	0	104
GLUTAMINE METABOLISM	42	20	0	0	0	20
PENTOSE PHOSPHATE PATHWAY	64	12	2	2	2	39
PORPHYRIN METABOLISM	51	17	0	0	0	26
MITOCHONDRIAL METABOLISM	608	349	1	35	0	360
OXIDATIVE PHOSPHORYLATION AND TCA CYCLE	232	179	0	0	0	109
MITOCHONDRIAL GENES	114	116	2	30	0	36
Signaling (rewirable)						
APOPTOSIS	584	246	34	40	57	401
NECROPTOSIS	242	118	0	0	0	188
FERROPTOSIS	193	65	17	19	0	110
PARTHANATOS	80	17	1	0	0	64
PYROPTOSIS	112	36	1	0	0	79
Execution (irreversible)						
MOMP REGULATION	630	319	19	48	17	396
MITOCHONDRIAL PERMEABILITY TRANSITION	57	36	0	0	0	33
CASPASES	318	158	5	5	12	221
RCD GENES	633	135	168	179	90	365
RCD GLOBAL MAP	**2657**	**1008**	**215**	**260**	**93**	**2020**

Table 2: Top contributing genes per module for Alzheimer and lung cancer datasets. Green: positively contributing genes, red: negatively contributing genes.

Module	Top Contributing genes AD	Top Contributing genes LC
MOMP REGULATION	*ATG5*, *VDAC3*, *CUL2*, *CYCS*, *HK1*, *MAPK6*, *BMF*, *RPS6KA1*, *MAPK10*, *VDAC2*	*DIABLO*, *RPS6KA1*, *CISH*, *CSNK2A1*, *C1QBP*, *FOXO1*, *PPP1CC*, *BCL2L11*, *SLC25A5*, *VDAC2*
STARVATION AUTOPHAGY	*CAB39*, *ATG5*, *MAPK6*, *MAPK8*, *ACACA*, *PINK1*, *RPS6KA1*, *CASP8*, *MTOR*, *ATG12*	*PARP1*, *SESN1*, *LDHA*, *BCL2L11*, *PI3KC3*, *RPS6KA1*, *PINK1*, *ATG3*, *ATG12*
GLUCOSE METABOLISM	*PFKM*, *PRKACB*, *PRKAA2*, *LDHA*, *NOTCH1*, *H6PD*, *ALDOA*	*PGK1*, *LDHA*, *ANAPC11M* *ALDOA*, *LDHC*, *PKM*, *ANAPC2*
FATTY ACID BIOSYNTHESIS	*PRKAA2*, *PPAT*, *CAB39*, *PRPS1*, *PRKACB*, *ACACA*	*ACLY*, *ACSS2*, *MLST8*, *PRPS1*, *PRPS2*
MITOCHONDRIAL METABOLISM	*SLC25A14*, *NDUFA9*, *FH*, *DLD*, *NDUFAF1*, *HK3*, *TNFRSF1A*, *ALOX15B*	UQCRH, ATP5G1, SLC25A10, CYC1, TACO1, NDUFAB1, PFKB2, RIPK3, SESN1, PLA2G4C
PYROPTOSIS	*IL18*, *CASP4*, *GBP2*, *CASP1*, *AIM2*	*CASP1*, *GBP2*, *IL18*, *CASP4*, *IL1B*
CASPASES	*YWHAG*, *MAPK8*, *MAPK6*, *CAB39*, *LMNA*, *HIP1*, *RIPK3*, *MTOR*	*G0S2*, *BIRC3*, *PIDD*, *FOXO1*, *RNF41*
DEPENDENCE RECEPTORS	*AATF*, *APPL2*, *PPP2CB*, *NGF*, *CARD8*, *NSMAF*	*PIK3CA*, *NEDD4*, *TRAF6*, *PPP2CB*, *NSMAF*
FERROPTOSIS	*NFE2L2*, *NQO1*, *FTL*, *ACSF2*, *SLC3A2*, *FTH1*	*GCLC*, *GCLM*, *GSR*, *MAFG*, *GSS*, *SLC3A2*
DEATH RECEPTOR PATHWAYS	*B4GALT6*, *GUCY1B3*, *CUL3*, *RBX1*, *RIPK3*, *HIF1A*, *NDUT5*, *CASP3*	*CYLD*, *PARP1*, *BRCA1*, *H2AFX*, *PRKDC*, *CARD8*, *STAT5A*, *FOXO1*, *MAGED1*, *TNFAIP3*
MITOCHONDRIAL PERMEABILITY TRANSITION	*SLC25A4*, *HK1*, *VDAC3*, *VDAC1*, *PPID*, *CKMT1A*, *VDAC2*	*PPID*, *CAPN2*, *VDAC2*, *SLC25A5*
MITOCHONDRIAL GENES	*ATP5C1*, *ATP5H*, *ATP5L*, *AIFM1*, *ATP5G1*, *NDUFB6*, *NDUFC2*, *ATP5A1*, *COX7A2*, *NDUFS4*	*ATP5G1*, *NDUFAB1*, *COX5B*, *ATP5B*, *NDUFB9*, *ATP5G3*, *COX6A1*, *COX6C*, *TACO1*, *COX8A*
PENTOSE PHOSPHATE PATHWAY	ACACB, NME4	*NME2*, *ACACB*, *RRM1*, *ACSS2*, *RRM2B*, *NME4*, *TXN*, *TP53*, *NME7*
NECROPTOSIS	B4GALT6, CUL3, RBX1, RIPK3, HK3, CASP10, PPP1CC	*GUCY1A3*, *H2AFX*, *PARP1*, *CFLAR*, *RIPK3*, *GUCY1A2*, *DNM1L*, *MLKL*, *NCF1*
GLUTAMINE METABOLISM	*GLS*, *GLS2*	*MLKL*, *RIPK3*, *RIPK1*, *PRPS1*
FAS RESPONSE	*CFLAR*, *CASP8*, *MLKL*,	*PTPN13*, *TNFSF10*, *MLKL*,

	GALNT14, *CASP10*	*CFLAR*, *RIPK1*, *SQSTM1*
TNF RESPONSE	*CYLD*, *MAP3K7*, *BIRC2*, *NSMAF*, *TAB2*	*CYLD*, *FLAD1*, *RNF11*, *PPP6C*, *CIAPIN1*, *RIPK1*, *CFLAR*
TRAIL RESPONSE	*CYLD*, *CASP8*, *MLKL*, *GALNT14*, *CASP10*	*MLKL*, *TNFAIP3*, *CFLAR*, *RIPK1*, *TNFRSF10D*
RCD GENES	*FBXO45*, *PKM*, *CDC42*, *ATG12*, *HSP90AA1*, *SIRT1*, *HIF1A*, *CASP3*, *BIRC2*	*KLF8*, *BCL2L11*, *STAT5A*, *PGK1*, *HUWE1*, *ALAS1*, *ENO1*, *NPM1*, *HSP90B1*, *ELK1*
APOPTOSIS	*RHOA*, *TCEB1*, *CYCS*, *SKP1*, *CCNB1*, *NKRF*, *BECN1*, *YWHAG*, *RPS6KA1*, *HIP1*	*DIABLO*, *STAT5A*, *RIPK3*, *CISH*, *RPS6KA1*, *HUWE1*, *C1QBP*, *BCL2L11*, *CDK6*, *PPP3R1*
DNA DAMAGE RESPONSE	*PPP2R1A*, *CAB39*, *CSNK2A1*, *NKRF*, *HUWE1*, *RNF8*, *PRKDC*	*H2AFX*, *RAD50*, *MRE11A*, *ACSS2*, *HUWE1*, *BARD1*, *NKRF*, *CANK2A1*, *PPARGC1A*, *APBB1*
PORPHYRIN METABOLISM	*UROD*, *COX10*, *UROS*, *CPOX*, *COX15*	*CPOX*, *ALAS1*, *HMBS*, *ALAS2*
ER STRESS	*DERL1*, *DERL2*, *HSPA9*, *ATP2A1*, *MAP3K5*, *MAP3K4*, *DNAJC3*, *VCP*, *EIF2S3*	*NLRC4*, *PDIA6*, *RYR2*, *NFKB1*, *PDIA4*, *DNAJB11*, *SEC61G*, *SEC61A1*, *CREB3L4*, *ITPR1*
ANTIOXIDANT RESPONSE	*NDUFS1*, *AIFM1*, *RBX1*, *CUL3*, *NDUFC2*, *NDUFAF1*, *COX7A2*, *NDUFS4*, *NDUFB5*, *COX6B2*	*UQCRH*, *MCL1*, *NDUFAB1*, *CYC1*, *COX5B*, *STAT5A*, *NDUFB9*, *COX6B1*, *COX4I2*, *COX6C*
OXIDATIVE PHOSPHORYLATION AND TCA CYCLE	*NDUFS1*, *ATP5H*, *SLC25A14*, *PARK2*, *IDH3B*, *NDUFC2*, *FH*, *ATP5G1*, *IDH3A*, *SLC1A5*	*ATP5B*, *NDUFAB1*, *COX5B*, *ATP5G3*, *COX8A*, *COX6C*, *COX6B1*, *FH*, *NDUFB10*, *COX5A*

Figure 1

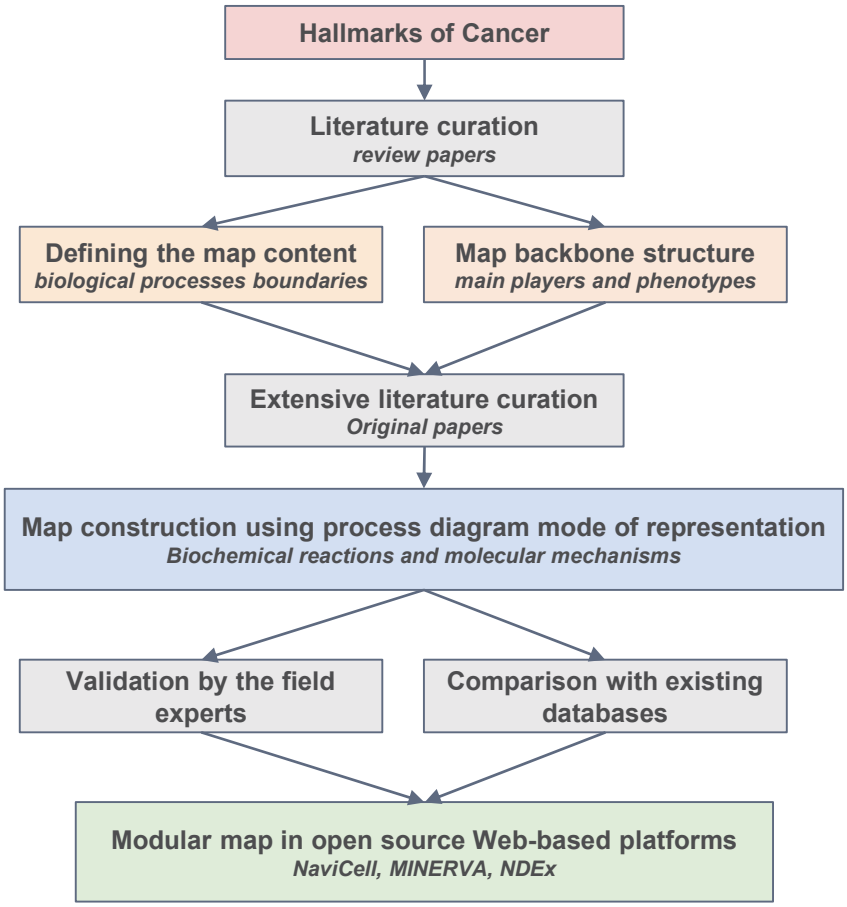
Hallmarks of Cancer
Literature curation
review papers
Defining the map content
biological processes boundaries
Map backbone structure
main players and phenotypes
Extensive literature curation
Original papers
Map construction using process diagram mode of representation
Biochemical reactions and molecular mechanisms
Validation by the field experts
Comparison with existing databases
Modular map in open source Web-based platforms
NaviCell, MINERVA, NDEx

Figure 2

A

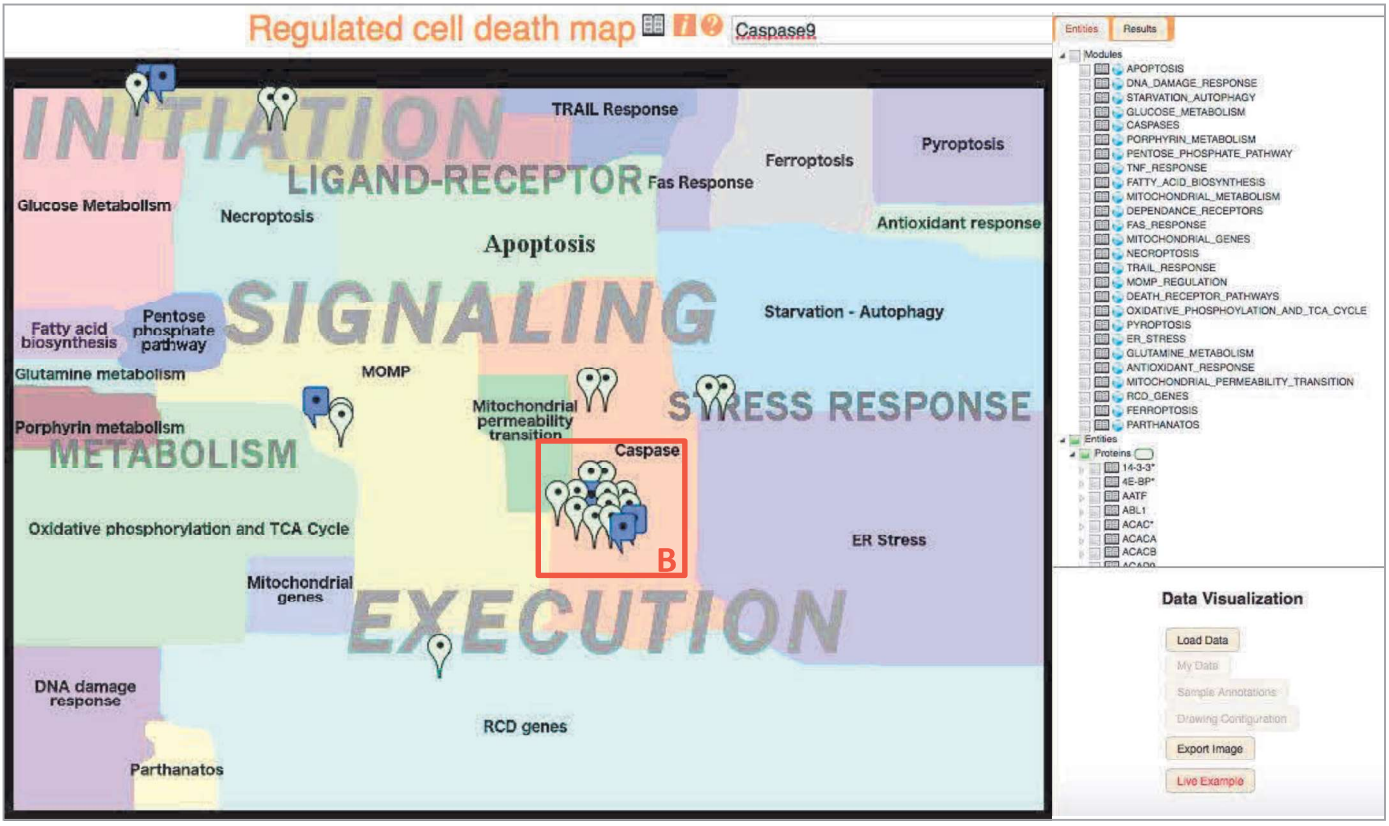
Regulated cell death map
Caspase9
INITIATION
LIGAND-RECEPTOR
SIGNALING
METABOLISM
STRESS RESPONSE
EXECUTION
TRAIL Response
Ferroptosis
Pyroptosis
Fas Response
Glucose Metabolism
Necroptosis
Antioxidant response
Apoptosis
Starvation - Autophagy
Fatty acid biosynthesis
Pentose phosphate pathway
Glutamine metabolism
MOMP
Mitochondrial permeability transition
Porphyrin metabolism
Caspase
Oxidative phosphorylation and TCA Cycle
ER Stress
Mitochondrial genes
DNA damage response
RCD genes
Parthanatos
B
Entities
Results
Modules
APOPTOSIS
DNA_DAMAGE_RESPONSE
STARVATION_AUTOPHAGY
GLUCOSE_METABOLISM
CASPASES
PORPHYRIN_METABOLISM
PENTOSE_PHOSPHATE_PATHWAY
TNF_RESPONSE
FATTY_ACID_BIOSYNTHESIS
MITOCHONDRIAL_METABOLISM
DEPENDANCE_RECEPTORS
FAS_RESPONSE
MITOCHONDRIAL_GENES
NECROPTOSIS
TRAIL_RESPONSE
MOMP_REGULATION
DEATH_RECEPTOR_PATHWAYS
OXIDATIVE_PHOSPHOYLATION_AND_TCA_CYCLE
PYROPTOSIS
ER_STRESS
GLUTAMINE_METABOLISM
ANTIOXIDANT_RESPONSE
MITOCHONDRIAL_PERMEABILITY_TRANSITION
RCD_GENES
FERROPTOSIS
PARTHANATOS
Entities
Proteins
14-3-3*
4E-BP*
AATF
ABL1
ACAC*
ACACA
ACACB
Data Visualization
Load Data
My Data
Sample Annotations
Drawing Configuration
Export Image
Live Example

B

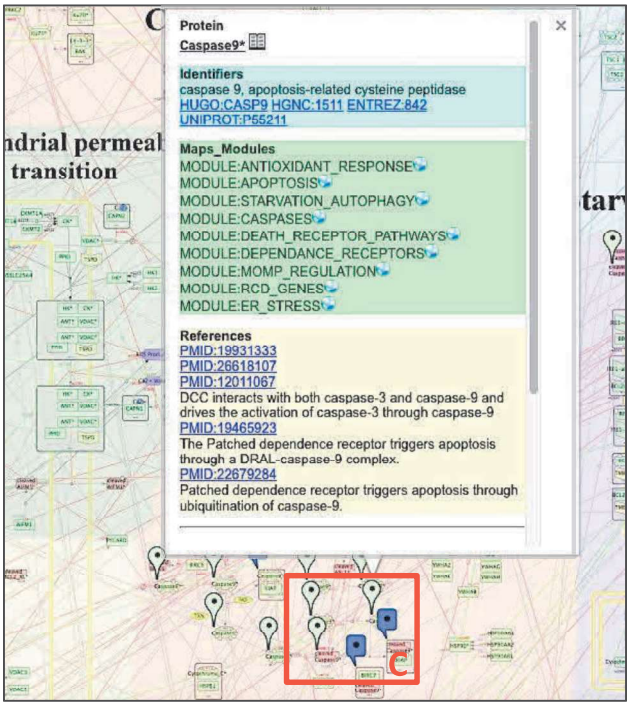
Protein
Caspase9*
Identifiers
caspase 9, apoptosis-related cysteine peptidase
HUGO:CASP9 HGNC:1511 ENTREZ:842
UNIPROT:P55211
Maps_Modules
MODULE:ANTIOXIDANT_RESPONSE
MODULE:APOPTOSIS
MODULE:STARVATION_AUTOPHAGY
MODULE:CASPASES
MODULE:DEATH_RECEPTOR_PATHWAYS
MODULE:DEPENDANCE_RECEPTORS
MODULE:MOMP_REGULATION
MODULE:RCD_GENES
MODULE:ER_STRESS
References
PMID:19931333
PMID:26618107
PMID:12011067
DCC interacts with both caspase-3 and caspase-9 and drives the activation of caspase-3 through caspase-9
PMID:19465923
The Patched dependence receptor triggers apoptosis through a DRAL-caspase-9 complex.
PMID:22679284
Patched dependence receptor triggers apoptosis through ubiquitination of caspase-9.
C

C

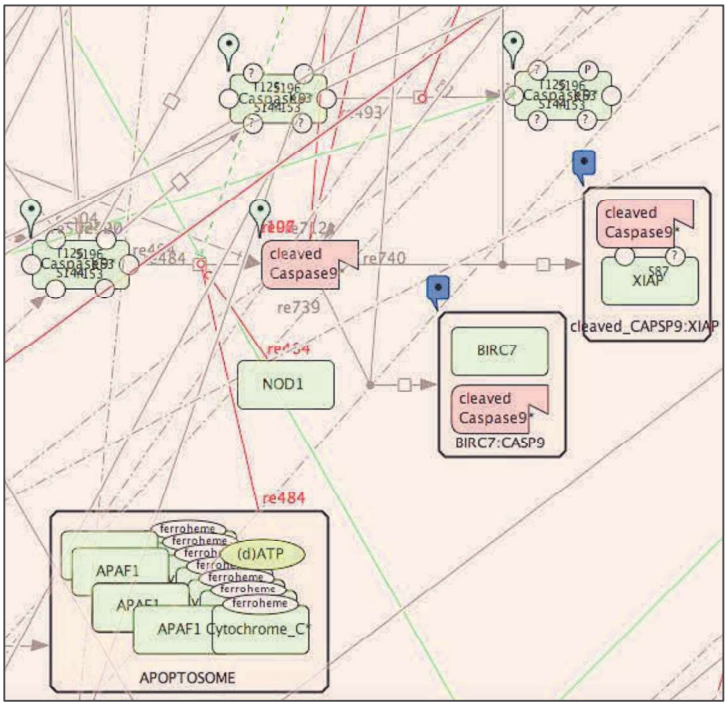
cleaved Caspase9
XIAP
cleaved_CAPSP9:XIAP
BIRC7
cleaved Caspase9
BIRC7:CASP9
NOD1
re739
re740
re484
APAF1
(d)ATP
Ferroheme
APAF1 Cytochrome_C*
APOPTOSOME

Figure 3

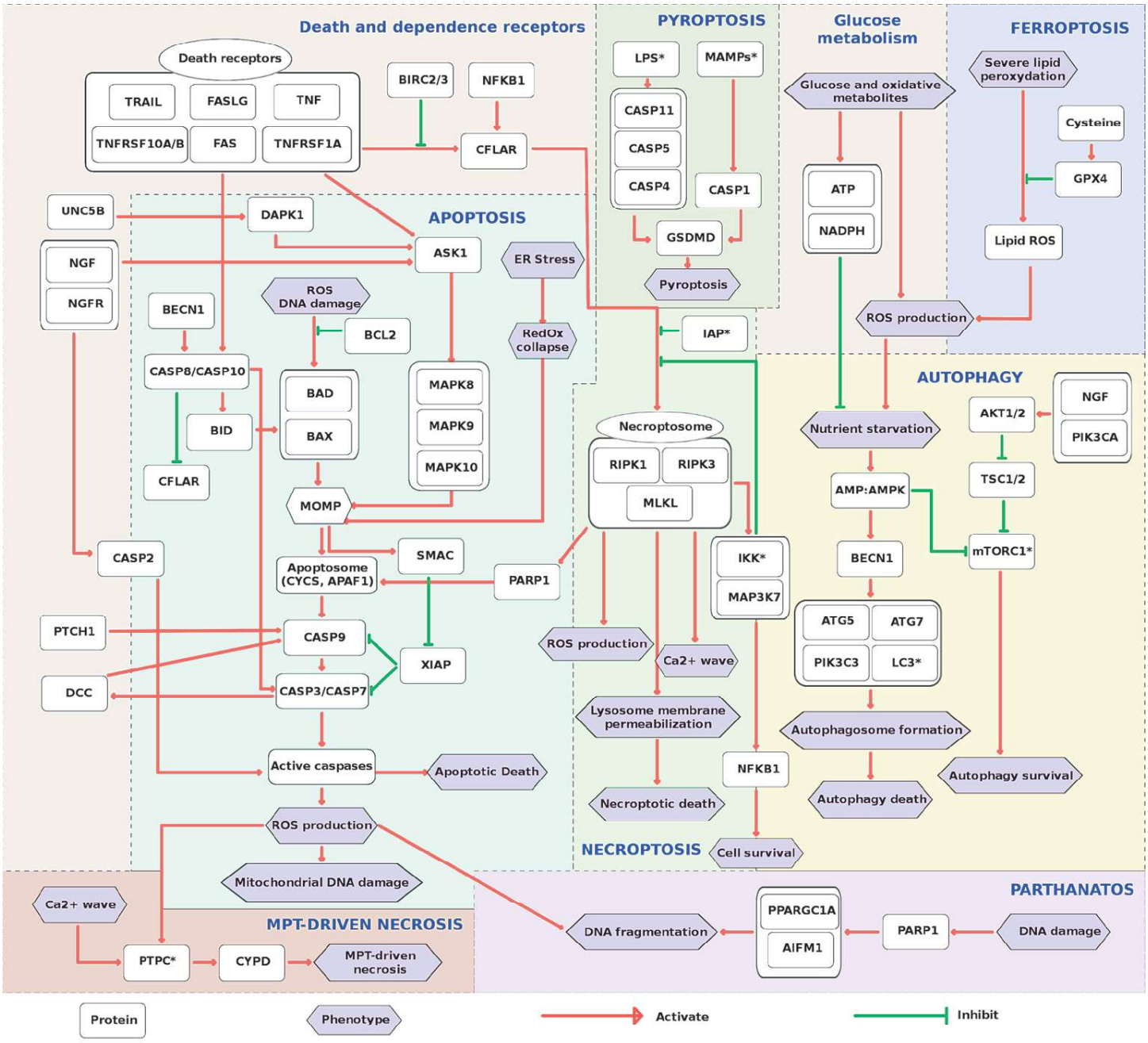
Death and dependence receptors
Death receptors
TRAIL
FASLG
TNF
TNFRSF10A/B
FAS
TNFRSF1A
BIRC2/3
NFKB1
CFLAR
UNC5B
DAPK1
APOPTOSIS
NGF
NGFR
ASK1
ER Stress
BECN1
ROS
DNA damage
BCL2
RedOx
collapse
CASP8/CASP10
BAD
BAX
MAPK8
MAPK9
MAPK10
BID
CFLAR
MOMP
CASP2
SMAC
Apoptosome
(CYCS, APAF1)
PARP1
PTCH1
CASP9
XIAP
DCC
CASP3/CASP7
Active caspases
Apoptotic Death
ROS production
Mitochondrial DNA damage
Ca2+ wave
MPT-DRIVEN NECROSIS
PTPC*
CYPD
MPT-driven
necrosis
PYROPTOSIS
LPS*
MAMPs*
CASP11
CASP5
CASP4
CASP1
GSDMD
Pyroptosis
IAP*
Necroptosome
RIPK1
RIPK3
MLKL
IKK*
MAP3K7
ROS production
Ca2+ wave
Lysosome membrane
permeabilization
NFKB1
Necroptotic death
NECROPTOSIS
Cell survival
Glucose
metabolism
Glucose and oxidative
metabolites
ATP
NADPH
ROS production
AUTOPHAGY
Nutrient starvation
AMP:AMPK
BECN1
ATG5
ATG7
PIK3C3
LC3*
Autophagosome formation
Autophagy death
AKT1/2
NGF
PIK3CA
TSC1/2
mTORC1*
Autophagy survival
FERROPTOSIS
Severe lipid
peroxydation
Cysteine
GPX4
Lipid ROS
PARTHANATOS
DNA fragmentation
PPARGC1A
AIFM1
PARP1
DNA damage
Protein
Phenotype
Activate
Inhibit

Figure 4

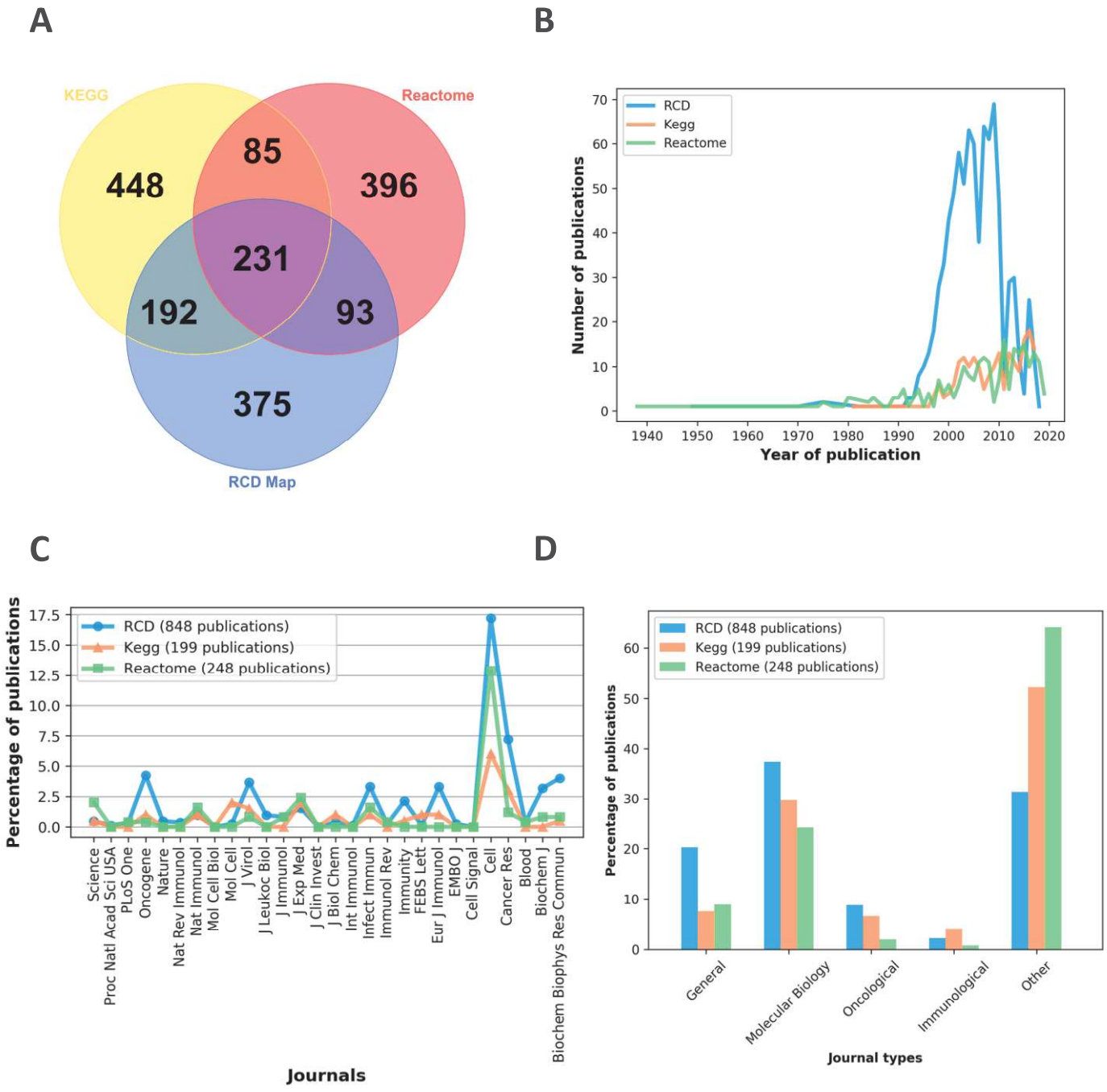
A
KEGG
Reactome
RCD Map
448
85
396
231
192
93
375
B
RCD
Kegg
Reactome
Number of publications
Year of publication
C
RCD (848 publications)
Kegg (199 publications)
Reactome (248 publications)
Percentage of publications
Journals
Science
Proc Natl Acad Sci USA
PLoS One
Oncogene
Nature
Nat Rev Immunol
Nat Immunol
Mol Cell Biol
Mol Cell
J Virol
J Leukoc Biol
J Immunol
J Exp Med
J Clin Invest
J Biol Chem
Int Immunol
Infect Immun
Immunol Rev
Immunity
FEBS Lett
Eur J Immunol
EMBO J
Cell Signal
Cell
Cancer Res
Blood
Biochem J
Biochem Biophys Res Commun
D
RCD (848 publications)
Kegg (199 publications)
Reactome (248 publications)
Percentage of publications
General
Molecular Biology
Oncological
Immunological
Other
Journal types

Figure 5

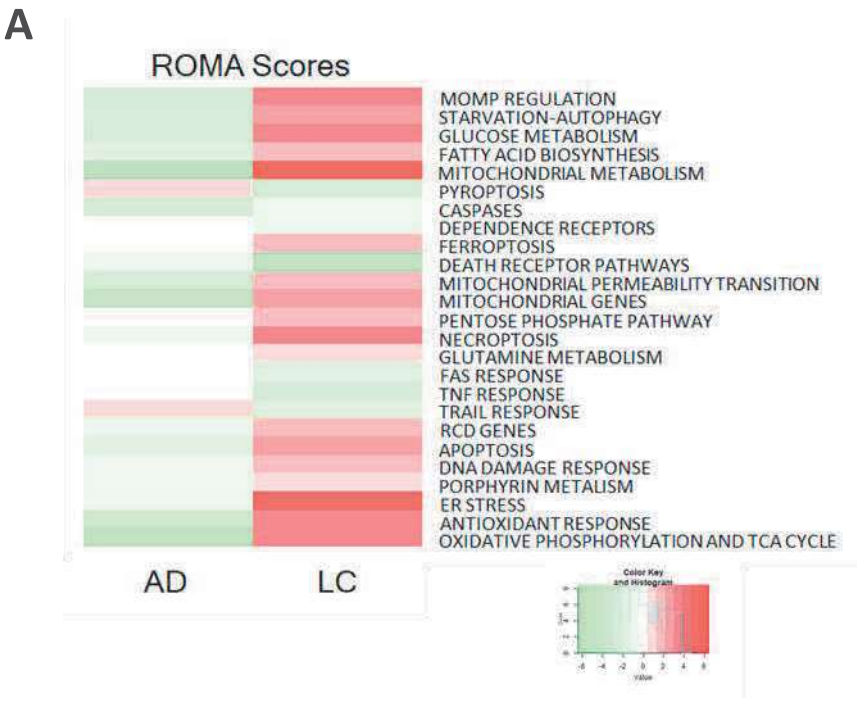
A
ROMA Scores
MOMP REGULATION
STARVATION-AUTOPHAGY
GLUCOSE METABOLISM
FATTY ACID BIOSYNTHESIS
MITOCHONDRIAL METABOLISM
PYROPTOSIS
CASPASES
DEPENDENCE RECEPTORS
FERROPTOSIS
DEATH RECEPTOR PATHWAYS
MITOCHONDRIAL PERMEABILITY TRANSITION
MITOCHONDRIAL GENES
PENTOSE PHOSPHATE PATHWAY
NECROPTOSIS
GLUTAMINE METABOLISM
FAS RESPONSE
TNF RESPONSE
TRAIL RESPONSE
RCD GENES
APOPTOSIS
DNA DAMAGE RESPONSE
PORPHYRIN METALISM
ER STRESS
ANTIOXIDANT RESPONSE
OXIDATIVE PHOSPHORYLATION AND TCA CYCLE
AD
LC
Color Key and Histogram
Value

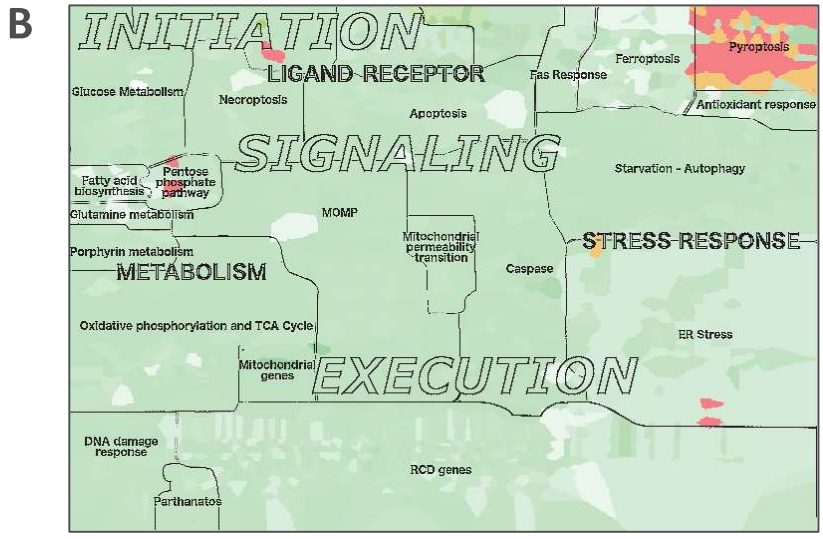
B
INITIATION
LIGAND-RECEPTOR
Glucose Metabolism
Necroptosis
Apoptosis
Fas Response
Ferroptosis
Pyroptosis
Antioxidant response
SIGNALING
Fatty acid biosynthesis
Pentose phosphate pathway
Glutamine metabolism
MOMP
Starvation - Autophagy
Porphyrin metabolism
METABOLISM
Mitochondrial permeability transition
Caspase
STRESS-RESPONSE
Oxidative phosphorylation and TCA Cycle
Mitochondrial genes
EXECUTION
ER Stress
DNA damage response
RCD genes
Parthanatos

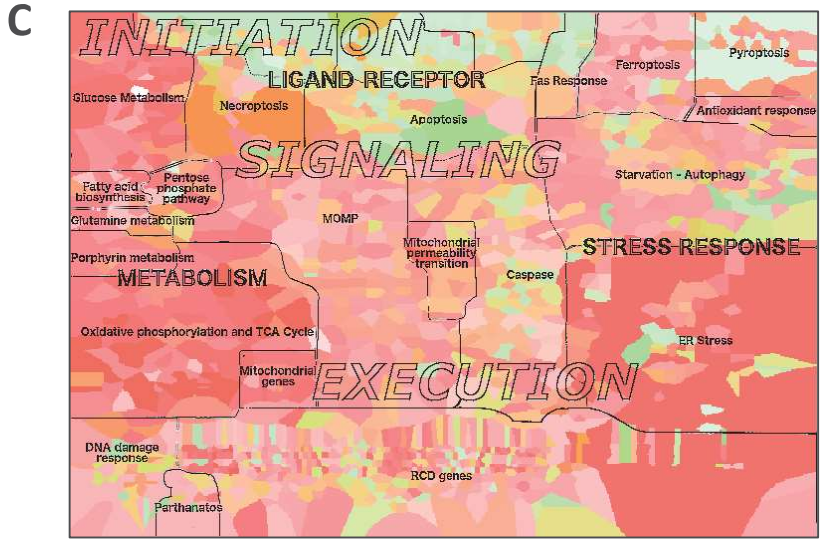
C
INITIATION
LIGAND-RECEPTOR
Glucose Metabolism
Necroptosis
Apoptosis
Fas Response
Ferroptosis
Pyroptosis
Antioxidant response
SIGNALING
Fatty acid biosynthesis
Pentose phosphate pathway
Glutamine metabolism
MOMP
Starvation - Autophagy
Porphyrin metabolism
METABOLISM
Mitochondrial permeability transition
Caspase
STRESS-RESPONSE
Oxidative phosphorylation and TCA Cycle
Mitochondrial genes
EXECUTION
ER Stress
DNA damage response
RCD genes
Parthanatos

Figure 6

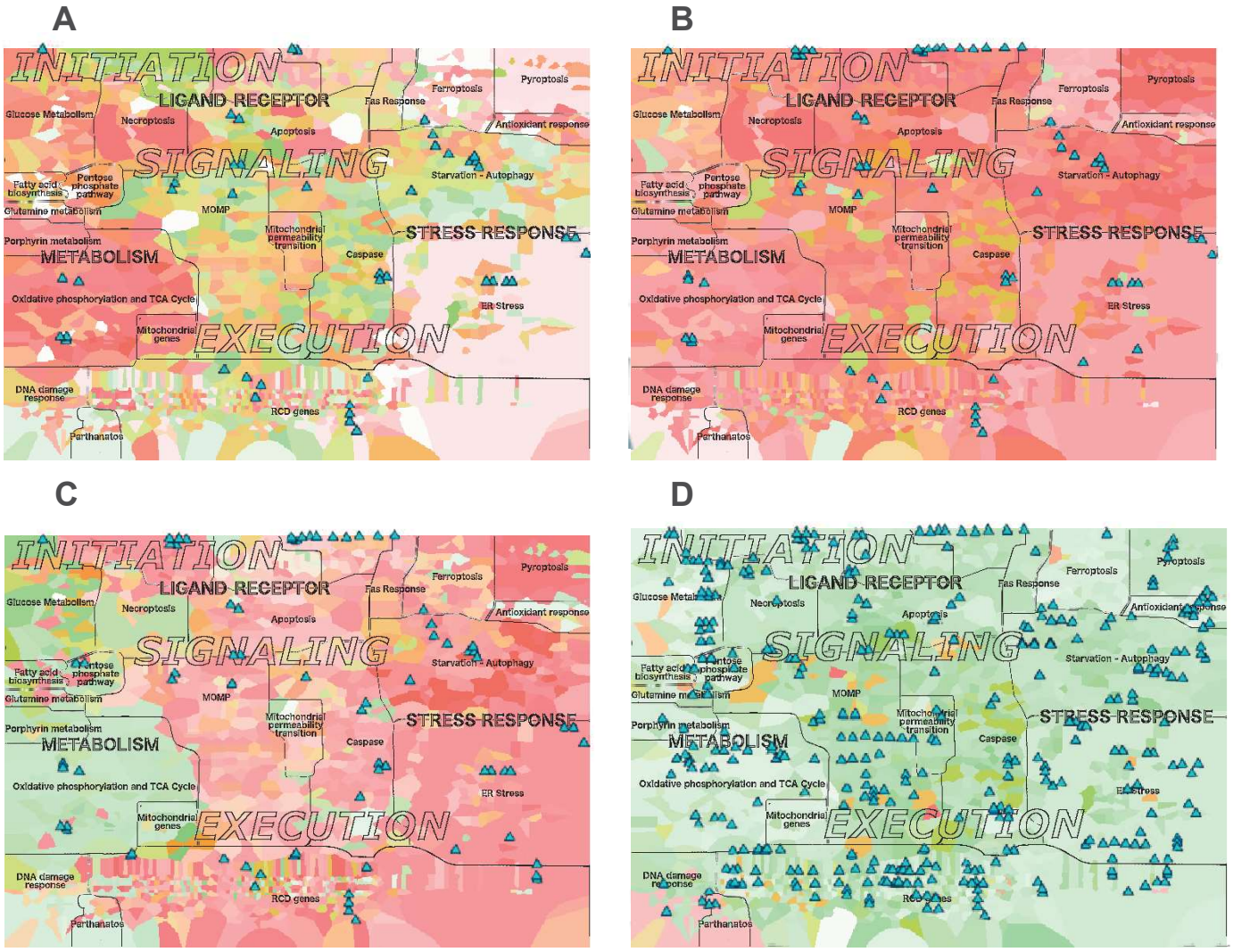
A
B
C
D
INITIATION
LIGAND RECEPTOR
SIGNALING
STRESS RESPONSE
METABOLISM
EXECUTION
Glucose Metabolism
Necroptosis
Fas Response
Ferroptosis
Pyroptosis
Apoptosis
Antioxidant response
Starvation - Autophagy
Fatty acid biosynthesis
Pentose phosphate pathway
Glutamine metabolism
MOMP
Mitochondrial permeability transition
Porphyrin metabolism
Caspase
Oxidative phosphorylation and TCA Cycle
ER Stress
Mitochondrial genes
DNA damage response
RCD genes
Parthanatos

E

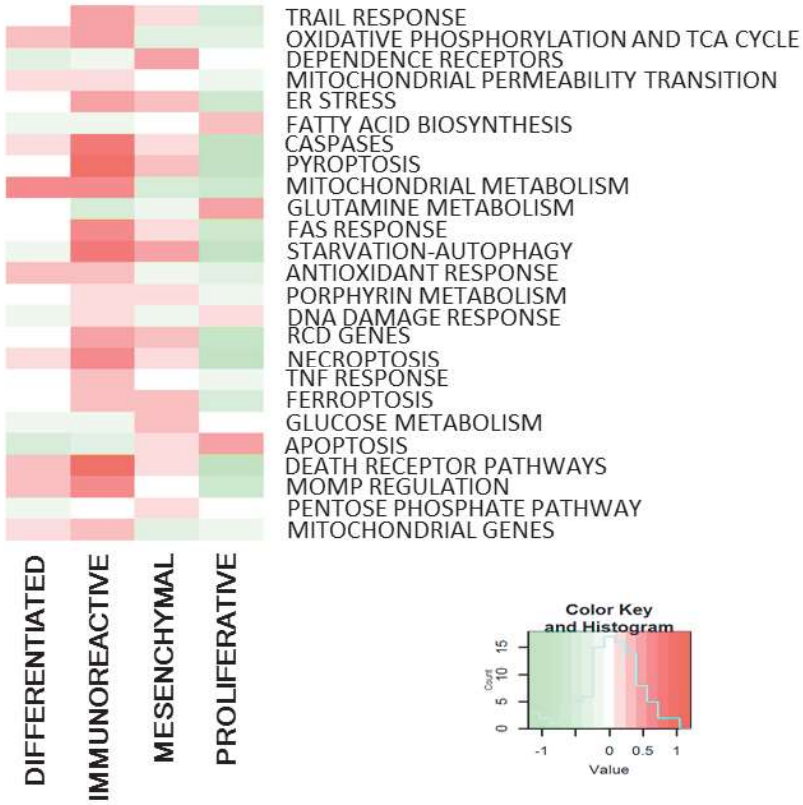
ROMA Scores
TRAIL RESPONSE
OXIDATIVE PHOSPHORYLATION AND TCA CYCLE
DEPENDENCE RECEPTORS
MITOCHONDRIAL PERMEABILITY TRANSITION
ER STRESS
FATTY ACID BIOSYNTHESIS
CASPASES
PYROPTOSIS
MITOCHONDRIAL METABOLISM
GLUTAMINE METABOLISM
FAS RESPONSE
STARVATION-AUTOPHAGY
ANTIOXIDANT RESPONSE
PORPHYRIN METABOLISM
DNA DAMAGE RESPONSE
RCD GENES
NECROPTOSIS
TNF RESPONSE
FERROPTOSIS
GLUCOSE METABOLISM
APOPTOSIS
DEATH RECEPTOR PATHWAYS
MOMP REGULATION
PENTOSE PHOSPHATE PATHWAY
MITOCHONDRIAL GENES
DIFFERENTIATED
IMMUNOREACTIVE
MESENCHYMAL
PROLIFERATIVE
Color Key and Histogram
Count
0
5
10
15
-1
0
0.5
1
Value

Supplementary Materials text

Content of the RCD map

Description of layers, functional meta-modules and modules

Layer Initiation (reversible)

Meta-module Ligand-Receptor

Module Death receptors are one of the most studied inputs of regulated cell death (RCD) and in particular apoptosis[1,2]. They can be split into two principal subtypes: the "canonical death receptors" triggering TNF, TNFSF10 (also known as TRAIL) and FAS (previously known as CD95) response[3,4] and dependence receptor[5].

Module "Canonical death receptors" are transmembrane receptors that can bind a ligand and then enhance recruitment of proteins. This protein can bind complexes including pro-apoptotic, pro-necroptotic and pro-survival components (as inhibitors). For example, TNF-TNFRSF1 complex will recruit adaptor protein TRADD witch can schematically bind FADD (potential binder of CASPCASP8, CASP8) itself, RIPK1 (inducer of necroptosis), cFLIP (encoded by *CFLAR*, inhibitors ofCASP8 and allowing switch between apoptosis to necroptosis[6]), etc. Depending on the cell context, the balance of each signal will be modulated, leading to the activation of one of the pathways (including pro-survival or no-signal)[1,7].

Module Dependence receptors have been described lately and are a group of receptors composed by more than a dozen of membrane receptors[5]. When they are bound by their ligand, they dimerize and inhibit the activation of caspases[8]. In absence of their ligand, they induce various pro-apoptotic pathways and eventually, CASPactivation. On the contrary to the canonical pathways, their pattern of activation and modulation are not similar between them. For example, DCC (for deleted in colorectal carcinoma) receptor in the absence of his ligand NTN1 (previously known as Netrin-1) is cleaved by CASP3 and this promotes his binding to APPL1 leading to CASPCASP9 and subsequent CASP3CASP activation, enhancing thus apoptosis[9].

During viral or bacterial infections, activation of the Pathogen-associated molecular patterns (PAMPs) can also activate NK kB pathway leading to pathogen clearance or cell death[10].

Meta-module Metabolism

Module General metabolism is one of the major RCD triggers, since it is at the centre of energy supply and its dysfunction could lead to reactive oxygen species (ROS) generation[11]. We represent on our map five particular pathways that have direct links to RCD through mechanisms described below: glucose metabolism, fatty acid biosynthesis, pentose phosphate pathway, glutamine metabolism and porphyrin metabolism[12].

Module Glucose metabolism is at the center of cell metabolism. Once glucose is incorporated into the cell, it gets phosphorylated in the cytoplasm, leading eventually to various reactions. More particularly,

glucose metabolism can cause ROS generation, inhibit starvation and also reverse the AMP/ATP ratio that is crucial for autophagy processes.

Module Fatty acid biosynthesis allows lipid synthesis through long-chain fatty acid assembly using Acetyl-coenzyme A, ATP and NADPH[12,13]. Acetyl-CoA is synthesized from citrate, a glycolysis end-product, ATP and coenzyme A. Lipid synthesis allows biomass production, energy supply and inhibition of starvation processes. The dysfunction in this process will lead to disordered energy supply and through AMPK pathway, will result in autophagy and eventually RCD.

Module Pentose phosphate pathway acts in parallel with glycolysis and aims to nucleotide synthesis[15]. The goal of this metabolic pathway is to synthesize materials for DNA and RNA synthesis. This pathway is very convenient for cell homeostasis as the same pathway could lead either to nucleotide synthesis or to energy production (going back to glycolysis pathway). In our case, detriment could lead to inappropriate DNA reparation, starvation and ROS generation.

Module Glutamine metabolism comprises a series of biochemical reactions that releases glutamate and ammonia [16]. Even small in the map, it is a major player in RCD. For instance, necroptosis recruits GLUL at the necrosome and activates it. Once activated, it can polymerise and catalyse the condensation of glutamate and ammonia to form glutamine.

Module Porphyrin metabolism takes place in both cytoplasm and mitochondria. It first starts in mitochondria with Succinyl-coenzyme A and Glycine catabolism and ends back into the mitochondria where the insertion of Fe2+ into the Protoporphyrin IX produces Ferroheme b. The lack of ferroheme leads to accumulation of cystoplasmic Fe2+ and thus ferroptosis. Heme deficiency is also a signal of persistent ER stress that induces cell death.

Module Mitochondrial metabolism is the main energy machinery of the cell and supplies ATP to the cell. It has numerous independent pathways of functioning.

Module Oxidative phosphorylation is the most efficient way to produce ATP in the cells. It uses a chain of redox reactions carried out by a series of protein complexes within the mitochondrial inner membrane. As a major energy supply, its substrates are mostly general metabolism products. Impairment will lead to starvation. However, if the chain is malfunctioning, ROS will be generated that might cause ER Stress and possibly, cell death.

Module TCA cycle is also known as Krebs cycle or citric acid cycle. Basically, it allows symbiosis between nutritional input, energy storage and the cell's needs. Nutrients are metabolised through glycolysis and other pathways – such as fatty acid pathway - and results into citrate and Acetyl-CoA generation. TCA cycle is thus an energy supplier and a way to generate precursors like NADH (essential to energy supply and Redox regulation). NAD depletion would, for example, lead to Parthanatos.

Module Mitochondrial genes are a set of several genes that are not located in the cell nucleus but in the mitochondria. Defect of one of these genes, implies severe cell dysfunction. These genes are responsible for numerous rare diseases.

Meta-module Stress response

Module DNA damage is a major intracellular clue that will trigger a signalling called the "DNA damage response". This response includes mostly an activation of genes implicated in controlling regulated cell death, in particular the p53 regulator factor which, once activated, translocates into the nucleus and activates the transcription of several targets, including pro-apoptotic proteins like BAX[17,18].

Module Antioxidant response aims to protect cellular structures from oxidative damage. ROS are endogenously produced by cells but trigger RCD if they persist or reach pathological concentrations[19], causing damages e.g. protein misfolding, mitochondrial DNA mutation, and lipid peroxidation. Pathological concentrations can be due to dysfunction of mitochondrial metabolism such as glucose metabolism, fatty acid biosynthesis, and mostly oxidative phosphorylation and TCA cycle[20,21]. We could distinguish two steps into antioxidant response: an immediate response to ROS aggression and a more delayed but also more persistent signal. Immediate response is performed by "classical" antioxidant enzymes i.e. a biochemical structure that can absorb electrons without damages, as for example bilirubin-biliverdin couple or GSH-GSSG couple. A more stable and persistent response is obtained through gene modulation by transcriptional activation of antioxidant response element (ARE). ROS prevent ubiquitination (and successive destruction) of NFELE2 (also known as NRFL2) transcriptional activator. When NFELE2 is co-activated with small MAF proteins (MafF, MafG, and MafK), can activate transcription of several genes, for example, MTOR, TXN, HMOX1, BAK1 genes.

The **Module Endoplasmic Reticulum (ER)** is a vast organelle with a protein folding function but also lipid and carbohydrate metabolism and Calcium storage. Endoplasmic reticulum stress can be caused by perturbation of Ca2+ homeostasis, redox imbalance, and accumulation of unfolded or misfolded proteins in the ER lumen. All these perturbations can induce RCD as described above. ER Integrity is in particular allowed by the unfolded protein response (UPR) and its three major genes PERK, ATF6 and IRE1 but also by autophagy and antioxidant response[22]. UPR is often triggered by altered environmental conditions or intracellular threats (as ROS or Calcium concentration variation) explaining why UPR often induces pro-survival or pro-death pathways concomitantly[23]. Cytosolic Ca+ elevation can activate members of the Calpain protein family that, in turn, can cleave many proteins - depending of the cell type and the Calpain subtype - as BID[24] and AIF[25] enhancing thus Mitochondrial dependent apoptosis[26]. Activated calpains can also translocate into the nucleus and trigger RCD through activation of major pro-death genes[27].

Module Autophagy is the basic catabolic mechanism that involves cell degradation of unnecessary or dysfunctional cellular components through lysosomal activity, supporting normally survival, however if the nutrient and energy starvation reaches a non-physiological threshold, this mechanism will lead to cell death[28]. The primary aim of Autophagy is to help the cell to cope a stress condition by inducing or delaying cell death. The process is under the control of roughly 30 autophagy related genes (ATG family) and characterized by autophagosome formation induced by class 3 phosphoinositide-3-kinase, the autophagy-related gene (Atg) 6 (also known as Beclin-1); forming the PI3KCIII complex, and ubiquitin-like conjugation reactions[2,29,30]. Eventually, through activation cascades, autolysosome formation is

completed with autophagosome and lysosome fusion[29]. Subsequently, the autolysosome content is degraded and released into the cytoplasm providing a source of nutrients but, if there are abnormalities in ATP consumption and production, it elicits cell death[28]. This survival decision and the general autophagy process are tightly linked to energetic sensors, such as MTOR, AMPK and PKA pathways. As an example, energetic rich conditions (amino acids, nutrients) will activate mTORC1 and thus inhibit autophagy whereas starvation and oxidative stress will activate AMPK pathway and consequently promote cell death[31]. Once autophagy is evoked, the cell needs to choose between a pro-survival or a pro-death autophagy. This choice is mainly determined by the ATP concentration and the ATP/ADP/AMP ratio[32]. Basically, if the cell has enough energy, i.e. a high ATP/ADP ratio, then survival autophagy is favoured. In the other cases, autophagy processes will lead to death through phosphatidylserine exposure. This regulation illustrates the interplay between autophagy, the cellular energetic state and the life or death balance[29]. In addition, as apoptosis and necroptosis, autophagy is modulated by transcriptional regulation such as miRNA[33]. This mechanism of cell death can occur also without energy supply[34,35].

Layer Signalling (rewireable)

Module Apoptosis

Apoptotic program is represented by extrinsic and intrinsic apoptosis pathways[2]. As mentioned previously, extrinsic apoptosis is activated by extracellular death signals, via engagement of transmembrane death receptors that induce cell signalling leading to apoptosis' execution[36,37]. Upon binding of lethal ligands to their corresponding death receptors (FASLG to FAS receptors[3], TNF to TNFRSF1A receptor or TNFSF10 to TNFRSF10A/B [4]) initiation of the corresponding cell signalling that leads to caspase cascade activation via caspase-8, 10 followed by CASP3, CASP6 and CASP7; activation that subsequently cleaves cell substrates and results in cell death[37,38]. Alternatively, the signal can propagate via cleaved BID ensuing mitochondrial outer membrane permeabilization (MOMP) and initiation of mitochondria-dependent apoptotic pathway via apoptosome formation (see below). In addition, the extrinsic pathways can be induced by dependence receptors that initiate apoptotic signalling when the specific ligands are below critical concentrations[5]. The signalling from death receptors as DCC or UNC5B propagates via MOMP-CASP9 pathway and converges with apoptotic executors' CASP3, CASP6 and CASP7 as well[8]. The variety of extracellular conditions as drugs, UV exposure, DNA damaging agents etc. can cause cell metabolic failure due to mitochondrial or ER dysfunction[20]. This leads to the accumulation of intracellular stress as high levels of DNA damage, ROS, NO, Ca2+ unfolded proteins or glutamate that trigger the mitochondria-dependent apoptosis pathway or intrinsic apoptosis pathway[18,39].

Module Necroptosis

The programmed necrosis or "**necroptosis**" can be initiated by different stimuli, as death receptors TNFR1, FAS, TRAIL[40,41], DNA damage signals transmitted via PARP-1 following genotoxic stress[42,43] and ROS. Necroptosis initiation relies on ubiquitination and phosphorylation of receptor-interacting protein kinase 1 (RIPK1) and receptor-interacting protein kinase 3 (RIPK3)[44]. RIPK1 can be recruited by death receptors, bind RIPK3 and form a complex with MLKL named "Necrosome" in the cytoplasm[45]. RIPK1 can also form a "Complex II" with FADD, caspase-8 and cFLIP leading to CASP8 activation and apoptosis. Formation of necrosome serves as a molecular platform for recruitment of downstream components, especially MLKL and also GLUL, GLUD1 and PYGL, and is thus essential for necroptosis[46]. The necrosome can also interact with different other components, explaining the subtle regulation of necroptosis. CASP8, FADD and cFLIP are in particular frequently contained in this complex. This model explains why these triggers will activate necroptosis only in the context of caspases inhibition, in the other case CASPCASP8 will be activated in the necrosome complex leading to apoptosis and inhibition of necroptosis by cleaving RIP1 and RIP3[2,7,44,46]. Several downstream processes can occur simultaneously to execute necroptosis: most importantly lysosomal membrane permeabilization (LMP), activation of calpains, generation of sphingosine via sphingomyelin metabolism, mitochondrial fission via Drp1 activation, intracellular release of Fe2+ and lipid peroxidation via PLA2[47,48]. There are mechanisms by which enhanced glycogenolysis, glycolysis and glutaminolysis can contribute to the acceleration of ROS generation by the respiratory chain in mitochondria[45]. Altogether, these processes lead to ATP reduction, mitochondrial and cytoplasmic ROS accumulation, promoting membrane permeabilization and disintegration of mitochondrial, lysosomal and plasma membranes, and finally, release of cell contents[47,49].

Module Ferroptosis has been recently described as a singular regulated way for the cell to die. As its name indicates, Ferroptosis is closely link to iron homeostasis. Accumulation of cytoplasmic iron ion generates oxidative stress and leads to oxidation of membrane lipids. Ferroptosis presents specific features, for example the ferroptotic cell will have normal nuclear size and uncondensed chromatin, opposite to apoptotic cell death. At the centre of Ferroptosis regulation, is iron metabolism and also redox homeostasis and as such, the redox enzymes as GSSG – GSH couple.

Module Parthanatos was described as a distinct regulated cell death in 2009[50]. Poly-ADP-ribose polymerase-1 (PARP-1) activation is the core of this pathway as its name would indicate so (PAR-*Thanatos*). PARP-1 is structured in three domains: A N-terminal DNA-binding site, a central modification domain (with phosphorylation sites) and a N-terminal catalytic domain. PARP-1 role is to maintain homeostasis and keep DNA integrity. PARP senses single strand DNA breaks and catalyses then PAR polymerization from a NAD+ component. At physiological concentrations, PAR polymer would bind to AIFM1, hence, triggering DNA condensation and its repair. However, if PARP1 is over-activated, meaning that there are too many DNA damages, PAR will also be transformed into ADP-ribose through PARG enzyme and then catalysed to AMP. PARP1 overactivation will lead to FAD depletion (by over synthesis

of PAR), ATP depletion associated to increased cytoplasmic AMP levels (and further MOMP activation). Finally, phosphatidylserine will be exposed at the cell membrane as a death signal.

Module Pyroptosis is a caspase-dependent cell death with extracellular inputs that are mostly derived from bacteria, viruses and toxins. NLPR3 can however be triggered by several cues including ROS production, Cathepsin, potassium efflux and mitochondrial DNA. There are several different signals and few different receptors (NLRP1, NLRC4, NLRP3, AIM2 and Pyrin) but the pathway is very similar. As in a classic manner, ligand binding to its receptor will induce its dimerization. Dimerized receptor will allow PYCARD protein binding that in turn dimerizes and recruits Caspase-1. Caspase-1 will then self-activate and consequently cleave GSMD, leading to Pyroptosis execution.

Layer Execution (irreversible)

Module MOMP

As detailed in the modules mitochondria metabolism and **MOMP regulation**, one of the critical points of cell death, and especially apoptosis, is the initiation of irreversible permeabilization of mitochondria (MOMP formation) and mitochondrial trans-membrane potential dissipation. This triggers a sequence of events including respiratory chain inhibition and release of mitochondrial proteins[51]. The mitochondrial and cytoplasmic proteins Cytochrome C, APAF and dATP, form the apoptosome and in coordination with DIABLO and HTRA2 promote CASPCASP9 activation followed by caspase3 activation and execution of apoptosis in particular through DNA fragmentation[36,46].

Module Mitochondrial permeability transition is a pathway parallel to MOMP formation. It involves the creation of a channel through the mitochondrial membranes with VDAC proteins. PTPC formation is triggered by ROS production and Ca2+ wave Ca2+ influx will also activate Calpain 1 that will be able to cleaved AIFM1 inside mitochondria. PTPC will then allow cleaved AIMF1 translocation into cytoplasm and transduction of a death signal. The change of electro-chemical gradient will also trigger MOMP activation.

Module Caspases are considered classical cell death players. One could distinguish between initiator caspases (as caspases 8, 9 and 10) and executioner caspases (as caspases 3, 6 and 7). Caspases are enzymes with a catalytic cleavage domain and binding domains. Caspases are activated upon cleavage, and then they can cleave other proteins. In regulated cell death, the canonical pathway starts when a ligand binds to a receptor (that have a caspase-binding domain), allowing receptor dimerization and further recruitment of two side-by-side caspases. These initiator caspases could activate to each other and secondly activate another executioner caspase. This CASPwill in turn, cleave other proteins and prompting damages to the cell.

Module RCD genes

One of the ultimate steps in cell death is gene expression modification and ultimately, for some cell death types, DNA fragmentation. Among all the transcriptional factors implicated in cell death, FOXO, E2F1, p73, p53, PPARGC1A, NRF, HIF1A, NFKB1 and MYC are the most well-known. All these transcriptional factors are activated by the previously described upstream modules.

References

1 Jin Z, El-Deiry WS. Overview of cell death signaling pathways. *Cancer Biol Ther* 2005; **4**: 139–163.

2 Galluzzi L, Vitale I, Abrams JM, Alnemri ES, Baehrecke EH, Blagosklonny M V *et al.* Molecular definitions of cell death subroutines: recommendations of the Nomenclature Committee on Cell Death 2012. *Cell Death Differ* 2012; **19**: 107–120.

3 Yurchenko M, Shlapatska LM, Sidorenko SP. The multilevel regulation of CD95 signaling outcome. *Exp Oncol* 2012; **34**: 153–159.

4 Gonzalvez F, Ashkenazi A. New insights into apoptosis signaling by Apo2L/TRAIL. *Oncogene* 2010; **29**: 4752–4765.

5 Thibert C, Fombonne J. Dependence receptors: mechanisms of an announced death. *Cell Cycle* 2010; **9**: 2085–2091.

6 Gong J, Kumar S a., Graham G, Kumar AP. FLIP: Molecular switch between apoptosis and necroptosis. *Mol Carcinog* 2014; **53**: 675–685.

7 Silke J, Vucic D. *IAP family of cell death and signaling regulators*. 1st ed. Elsevier Inc., 2014 doi:10.1016/B978-0-12-801430-1.00002-0.

8 Goldschneider D, Mehlen P. Dependence receptors: a new paradigm in cell signaling and cancer therapy. *Oncogene* 2010; **29**: 1865–1882.

9 Mehlen P, Tauszig-delamasure S. Dependence receptors and colorectal cancer. 2014; : 1821–1829.

10 Medzhitov R, Janeway CA. Decoding the patterns of self and nonself by the innate immune system. *Science* 2002; **296**: 298–300.

11 Macfarlane M, Robinson GL, Cain K. Glucose—a sweet way to die. 2012; : 3919–3925.

12 Magtanong L, Ko PJ, Dixon SJ. Emerging roles for lipids in non-apoptotic cell death. *Cell Death Differ* 2016; **23**: 1099–1109.

13 Agmon E, Stockwell BR. Lipid homeostasis and regulated cell death. *Curr Opin Chem Biol* 2017; **39**: 83–89.

14 Zeng Z, Huang Q, Shu Z, Liu P, Chen S, Pan X *et al.* Effects of short-chain acyl-CoA dehydrogenase on cardiomyocyte apoptosis. *J Cell Mol Med* 2016; **20**: 1381–1391.

15 Jiang P, Du W, Wu M. Regulation of the pentose phosphate pathway in cancer. *Protein Cell* 2014; **5**: 592–602.

16 Lampa M, Arlt H, He T, Ospina B, Reeves J, Zhang B *et al.* Glutaminase is essential for the growth of triple-negative breast cancer cells with a deregulated glutamine metabolism pathway and its

suppression synergizes with mTOR inhibition. *PLoS One* 2017; **12**: e0185092.

17 Miyashita T, Reed JC. Tumor suppressor p53 is a direct transcriptional activator of the human bax gene. *Cell* 1995; **80**: 293–9.

18 Brinkmann K, Schell M, Hoppe T, Kashkar H. Regulation of the DNA damage response by ubiquitin conjugation. *Front Genet* 2015; **6**: 1–15.

19 Singh M, Sharma H, Singh N. Hydrogen peroxide induces apoptosis in HeLa cells through mitochondrial pathway. *Mitochondrion* 2007; **7**: 367–73.

20 Sinha K, Das J, Pal PB, Sil PC. Oxidative stress: The mitochondria-dependent and mitochondria-independent pathways of apoptosis. *Arch Toxicol* 2013; **87**: 1157–1180.

21 Fogg VC, Lanning NJ, Mackeigan JP. Mitochondria in cancer: at the crossroads of life and death. 2012; **30**: 526–539.

22 Senft D, Ronai Z a. UPR, autophagy, and mitochondria crosstalk underlies the ER stress response. *Trends Biochem Sci* 2015; **40**: 141–148.

23 Rutkowski DT, Hegde RS. Regulation of basal cellular physiology by the homeostatic unfolded protein response. *J Cell Biol* 2010; **189**: 783–794.

24 Vindis C, Elbaz M, Escargueil-Blanc I, Augé N, Heniquez A, Thiers J-C *et al.* Two distinct calcium-dependent mitochondrial pathways are involved in oxidized LDL-induced apoptosis. *Arterioscler Thromb Vasc Biol* 2005; **25**: 639–45.

25 Chen Q, Paillard M, Gomez L, Ross T, Hu Y, Xu A *et al.* Activation of mitochondrial μ-calpain increases AIF cleavage in cardiac mitochondria during ischemia-reperfusion. *Biochem Biophys Res Commun* 2011; **415**: 533–8.

26 Smith MA, Schnellmann RG. Calpains, mitochondria, and apoptosis. *Cardiovasc Res* 2012; **96**: 32–7.

27 Chang H, Sheng J-J, Zhang L, Yue Z-J, Jiao B, Li J-S *et al.* ROS-Induced Nuclear Translocation of Calpain-2 Facilitates Cardiomyocyte Apoptosis in Tail-Suspended Rats. *J Cell Biochem* 2015. doi:10.1002/jcb.25176.

28 Loos B, Engelbrecht AM, Lockshin RA, Klionsky DJ, Zakeri Z. The variability of autophagy and cell death susceptibility: Unanswered questions. *Autophagy* 2013; **9**: 1270–1285.

29 Fulda S, Kögel D. Cell death by autophagy: emerging molecular mechanisms and implications for cancer therapy. *Oncogene* 2015; : 1–9.

30 Zhi X, Zhong Q. Autophagy in cancer. *F1000Prime Rep* 2015; **7**: 1–12.

31 Naponelli V, Modernelli a., Bettuzzi S, Rizzi F. Roles of Autophagy Induced by Natural Compounds in Prostate Cancer. *Biomed Res Int* 2015; **2015**: 1–14.

32 Russell RC, Yuan H-X, Guan K-L. Autophagy regulation by nutrient signaling. *Cell Res* 2014; **24**: 42–57.

33 Frankel LB, Lund AH. MicroRNA regulation of autophagy. *Carcinogenesis* 2012; **33**: 2018–2025.

34 Chaabane W, User SD, El-Gazzah M, Jaksik R, Sajjadi E, Rzeszowska-Wolny J *et al.* Autophagy, apoptosis, mitoptosis and necrosis: interdependence between those pathways and effects on cancer. *Arch Immunol Ther Exp* 2013; **61**: 43–58.

35 Reyjal J, Cormier K, Turcotte S. Autophagy and cell death to target cancer cells: exploiting synthetic lethality as cancer therapies. *Adv Exp Med Biol* 2014; **772**: 167–188.

36 Goldar S, Khaniani MS, Derakhshan SM. Molecular Mechanisms of Apoptosis and Roles in Cancer Development and Treatment. 2015; **16**: 2129–2144.

37 Schulze-Osthoff K, Ferrari D, Los M, Wesselborg S, Peter ME. Apoptosis signaling by death receptors. *Eur J Biochem* 1998; **254**: 439–459.

38 Riedl SJ, Shi Y. Molecular mechanisms of CASPregulation during apoptosis. *Nat Rev Mol Cell Biol* 2004; **5**: 897–907.

39 Kroemer G, Dallaporta B, Resche-Rigon M. The mitochondrial death/life regulator in apoptosis and necrosis. *Annu Rev Physiol* 1998; **60**: 619–42.

40 Holler N, Zaru R, Micheau O, Thome M, Attinger A, Valitutti S *et al.* Fas triggers an alternative, caspase-8-independent cell death pathway using the kinase RIP as effector molecule. *Nat Immunol* 2000; **1**: 489–495.

41 Meurette O, Rebillard A, Huc L, Le Moigne G, Merino D, Micheau O *et al.* TRAIL induces receptor-interacting protein 1-dependent and caspase-dependent necrosis-like cell death under acidic extracellular conditions. *Cancer Res* 2007; **67**: 218–226.

42 Surova O, Zhivotovsky B. Various modes of cell death induced by DNA damage. *Oncogene* 2013; **32**: 3789–3797.

43 Virag L, Robaszkiewicz A, Rodriguez-Vargas JM, Oliver FJ. Poly(ADP-ribose) signaling in cell death. *Mol Asp Med* 2013; **34**: 1153–1167.

44 Almagro MC De, Vucic D. Necroptosis: Pathway diversity and characteristics. *Semin Cell Dev Biol* 2015; **1**: 1–7.

45 Christofferson DE, Yuan J. Necroptosis as an alternative form of programmed cell death. *Curr Opin Cell Biol* 2010; **22**: 263–268.

46 Lalaoui N, Lindqvist LM, Sandow JJ, Ekert PG. The molecular relationships between apoptosis, autophagy and necroptosis. *Semin Cell Dev Biol* 2015. doi:10.1016/j.semcdb.2015.02.003.

47 Vandenabeele P, Galluzzi L, Vanden Berghe T, Kroemer G. Molecular mechanisms of necroptosis: an ordered cellular explosion. *Nat Rev Mol Cell Biol* 2010; **11**: 700–714.

48 Yamashima T, Oikawa S. The role of lysosomal rupture in neuronal death. *Prog Neurobiol* 2009; **89**: 343–358.

49 Fulda S. The mechanism of necroptosis in normal and cancer cells. *Cancer Biol Ther* 2013; **14**. doi:26428 [pii].

50 David KK, Andrabi SA, Dawson TM, Dawson VL. Parthanatos, a messenger of death. *Front Biosci (Landmark Ed* 2009; **14**: 1116–28.

51 Galluzzi L, Kepp O, Trojel-Hansen C, Kroemer G. Mitochondrial control of cellular life, stress, and death. *Circ Res* 2012; **111**: 1198–1207.

Supplemental Figure 1

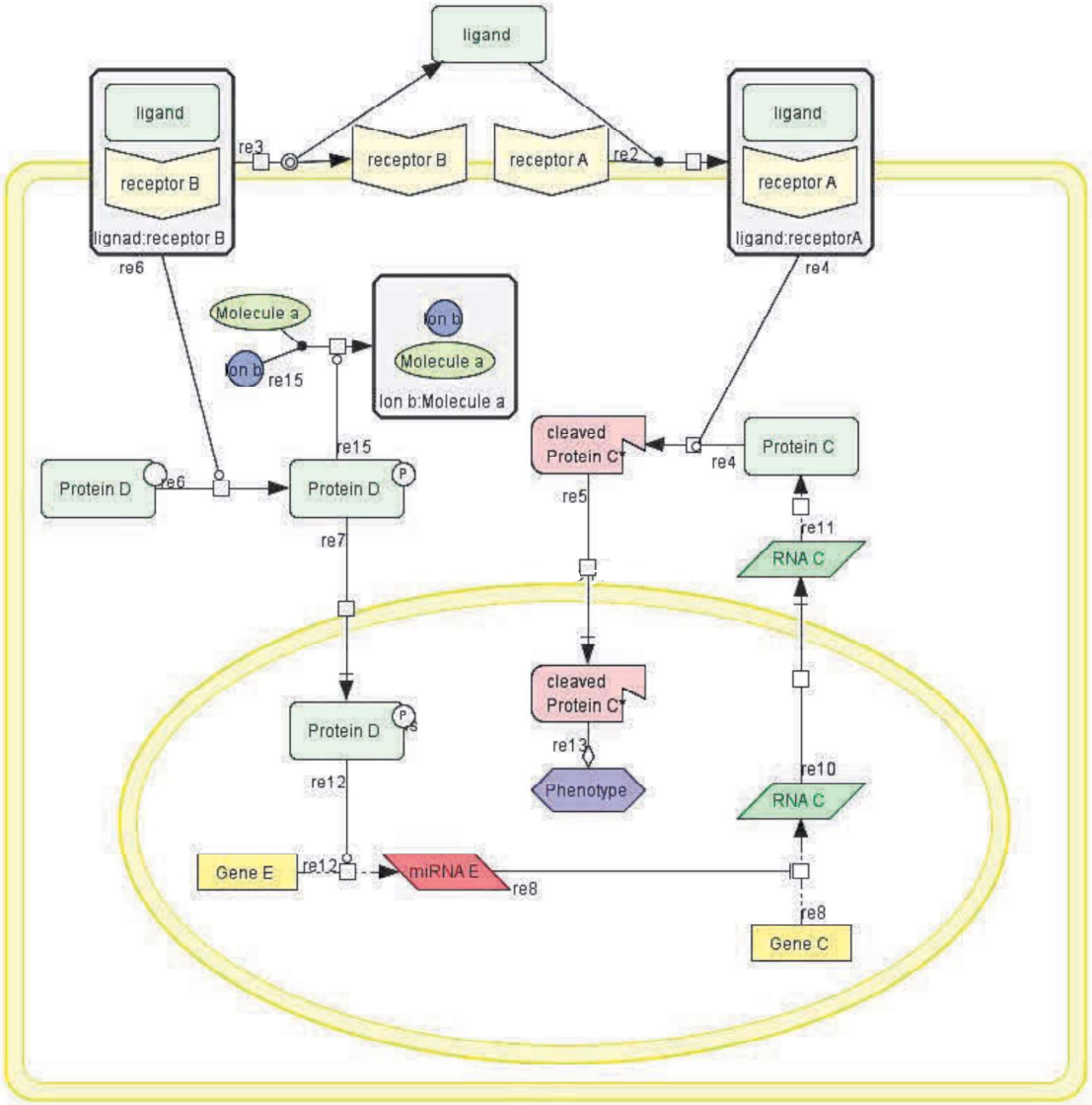

Supplemental Figure 2

Protein Caspase9*

Identifiers
caspase 9, apoptosis-related cysteine peptidase
HUGO:CASP9 HGNC:1511 ENTREZ:842 UNIPROT:P55211

Maps_Modules
MODULE:ANTIOXIDANT_RESPONSE
MODULE:APOPTOSIS
MODULE:STARVATION_AUTOPHAGY
MODULE:CASPASES
MODULE:DEATH_RECEPTOR_PATHWAYS
MODULE:DEPENDANCE_RECEPTORS
MODULE:MOMP_REGULATION
MODULE:RCD_GENES
MODULE:ER_STRESS

References
PMID:19931333
PMID:26618107
PMID:12011067
DCC interacts with both caspase-3 and caspase-9 and drives the activation of caspase-3 through caspase-9
PMID:19465923
The Patched dependence receptor triggers apoptosis through a DRAL-caspase-9 complex.
PMID:22679284
Patched dependence receptor triggers apoptosis through ubiquitination of caspase-9.

Modifications:

In compartment: Cytoplasm

1. Caspase9*@Cytoplasm
2. Caspase9*|K63_ubi@Cytoplasm
3. Caspase9*|S196_unk|S144_unk|Y153_unk@Cytoplasm
4. Caspase9*|S196_unk|T125_unk|S144_unk@Cytoplasm
5. Caspase9*|S196_unk|T125_unk|Y153_unk@Cytoplasm
6. Caspase9*|T125_unk|S144_unk|Y153_unk@Cytoplasm
7. Caspase9*|S196_pho|T125_unk|S144_unk|Y153_unk@Cytoplasm
8. Caspase9*|S196_unk|T125_pho|S144_unk|Y153_unk@Cytoplasm
9. Caspase9*|S196_unk|T125_unk|S144_pho|Y153_unk@Cytoplasm
10. Caspase9*|S196_unk|T125_unk|S144_unk|Y153_pho@Cytoplasm
11. Caspase9*|S196_unk|T125_unk|S144_unk|Y153_unk@Cytoplasm
12. Caspase9*|S196_unk|T125_unk|S144_unk|Y153_unk|ubi@Cytoplasm
13. Caspase9*|S196_unk|T125_unk|S144_unk|Y153_unk|-SNO@Cytoplasm

In compartment: Mitochondrial intermembrane space

1. Caspase9*@Mitochondrial intermembrane space

Participates in complexes:

In compartment: Cytoplasm

1. Caspase9*|S196_unk|T125_unk|S144_unk|Y153_unk:XIAP|S87_unk|hm2@Cytoplasm
2. APPL2:Caspase9*:Cleaved DCC*@Cytoplasm

In compartment: Mitochondrial intermembrane space

1. Caspase9*:HAX1@Mitochondrial intermembrane space

Participates in reactions:

As Reactant or Product:

1. Caspase9*|S196_unk|T125_unk|S144_unk|Y153_unk@Cytoplasm + NO@Cytoplasm → Caspase9*|S196_unk|T125_unk|S144_unk|Y153_unk|-SNO@Cytoplasm
2. Caspase9*@Mitochondrial intermembrane space + HAX1@Mitochondrial intermembrane space → Caspase9*:HAX1@Mitochondrial intermembrane space
3. Caspase9*@Mitochondrial intermembrane space + H_sub_2_endsub_O_sub_2_endsub_@Mitochondrial intermembrane space → s934
4. APPL2:Caspase9*:Cleaved DCC*@Cytoplasm → APPL2:Cleaved DCC*:cleaved~Caspase9*@Cytoplasm
5. APPL2@Cytoplasm + Cleaved DCC*@Cytoplasm + Caspase9*@Cytoplasm → APPL2:Caspase9*:Cleaved DCC*@Cytoplasm
6. Caspase9*@Cytoplasm → Caspase9*|K63_ubi@Cytoplasm
7. rCaspase9*@Nucleus → Caspase9*@Cytoplasm
8. Caspase9*@Cytoplasm → cleaved~Caspase9*@Cytoplasm
9. Caspase9*@Cytoplasm → cleaved~Caspase9*@Cytoplasm
10. Caspase9*|T125_unk|S144_unk|Y153_unk@Cytoplasm → Caspase9*|S196_pho|T125_unk|S144_unk|Y153_unk@Cytoplasm
11. Caspase9*@Cytoplasm → Caspase9*|T125_unk|S144_unk|Y153_unk@Cytoplasm
12. Caspase9*|S196_unk|T125_unk|Y153_unk@Cytoplasm → Caspase9*|S196_unk|T125_unk|S144_pho|Y153_unk@Cytoplasm
13. Caspase9*|S196_unk|T125_unk|S144_pho|Y153_unk@Cytoplasm → Caspase9*|S196_unk|T125_unk|Y153_unk@Cytoplasm
14. Caspase9*@Cytoplasm → Caspase9*|S196_unk|T125_unk|Y153_unk@Cytoplasm
15. Caspase9*|S196_unk|S144_unk|Y153_unk@Cytoplasm → Caspase9*|S196_unk|T125_pho|S144_unk|Y153_unk@Cytoplasm
16. Caspase9*|S196_unk|T125_pho|S144_unk|Y153_unk@Cytoplasm → Caspase9*|S196_unk|S144_unk|Y153_unk@Cytoplasm
17. Caspase9*@Mitochondrial intermembrane space → Caspase9*@Cytoplasm
18. Caspase9*@Cytoplasm → Caspase9*|S196_unk|S144_unk|Y153_unk@Cytoplasm
19. Caspase9*|S196_unk|T125_unk|S144_unk@Cytoplasm → Caspase9*|S196_unk|T125_unk|S144_unk|Y153_pho@Cytoplasm
20. Caspase9*@Cytoplasm → Caspase9*|S196_unk|T125_unk|S144_unk@Cytoplasm
21. Caspase9*|S196_unk|T125_unk|S144_unk|Y153_pho@Cytoplasm → cleaved~Caspase9*@Cytoplasm
22. Caspase9*@Cytoplasm → Caspase9*|S196_unk|T125_unk|S144_unk|Y153_unk@Cytoplasm
23. XIAP|S87_unk@Cytoplasm + Caspase9*|S196_unk|T125_unk|S144_unk|Y153_unk@Cytoplasm → Caspase9*|S196_unk|T125_unk|S144_unk|Y153_unk:XIAP|S87_
24. Caspase9*|S196_unk|T125_unk|S144_unk|Y153_unk@Cytoplasm → degraded
25. Caspase9*|S196_unk|T125_unk|S144_unk|Y153_unk@Cytoplasm → Caspase9*|S196_unk|T125_unk|S144_unk|Y153_unk|ubi@Cytoplasm
26. Caspase9*|S196_unk|T125_unk|S144_unk|Y153_unk|ubi@Cytoplasm → degraded
27. rCaspase9*@Nucleus → Caspase9*@Cytoplasm

Supplemental Figure 3A

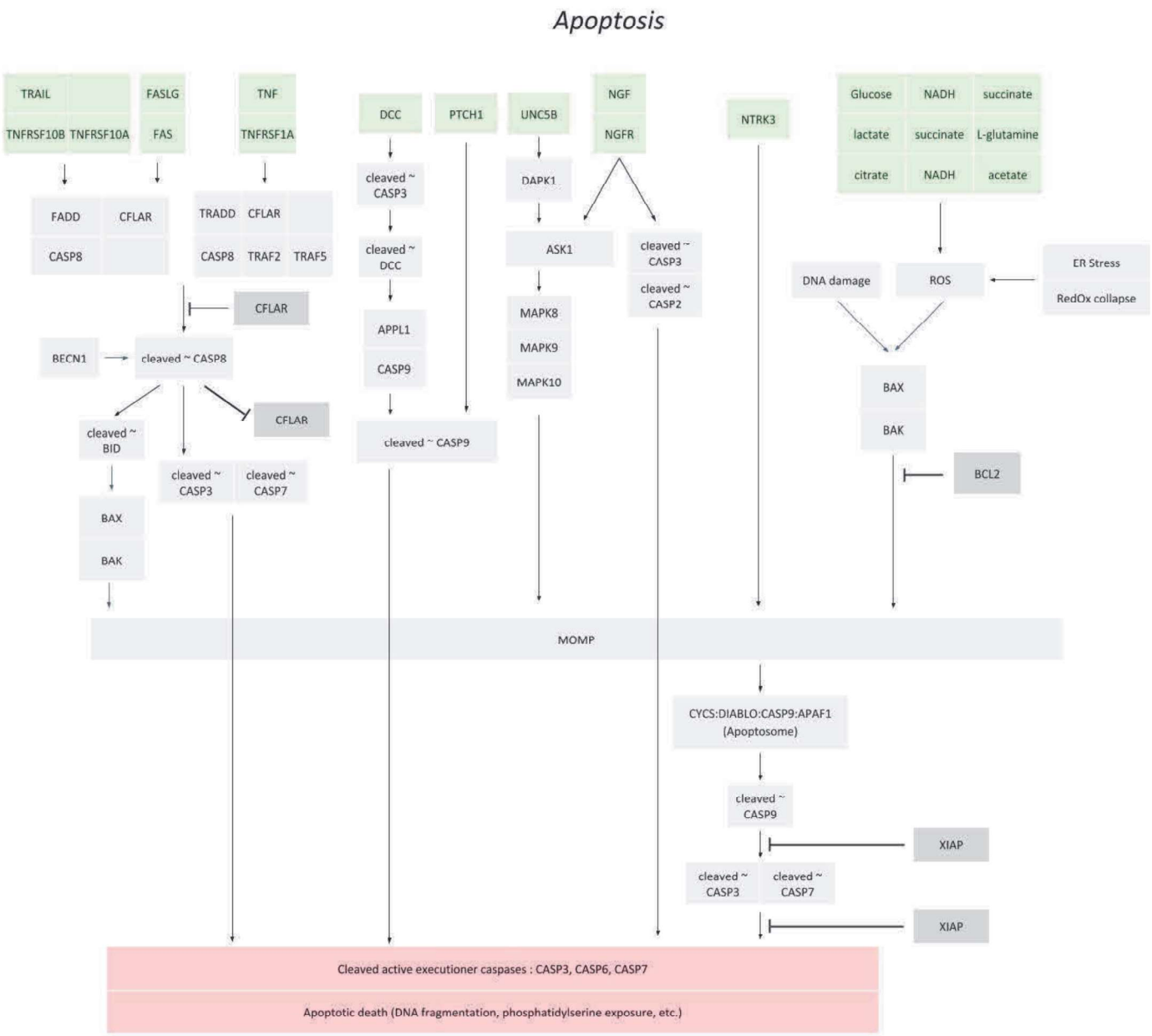

Supplemental Figure 3B

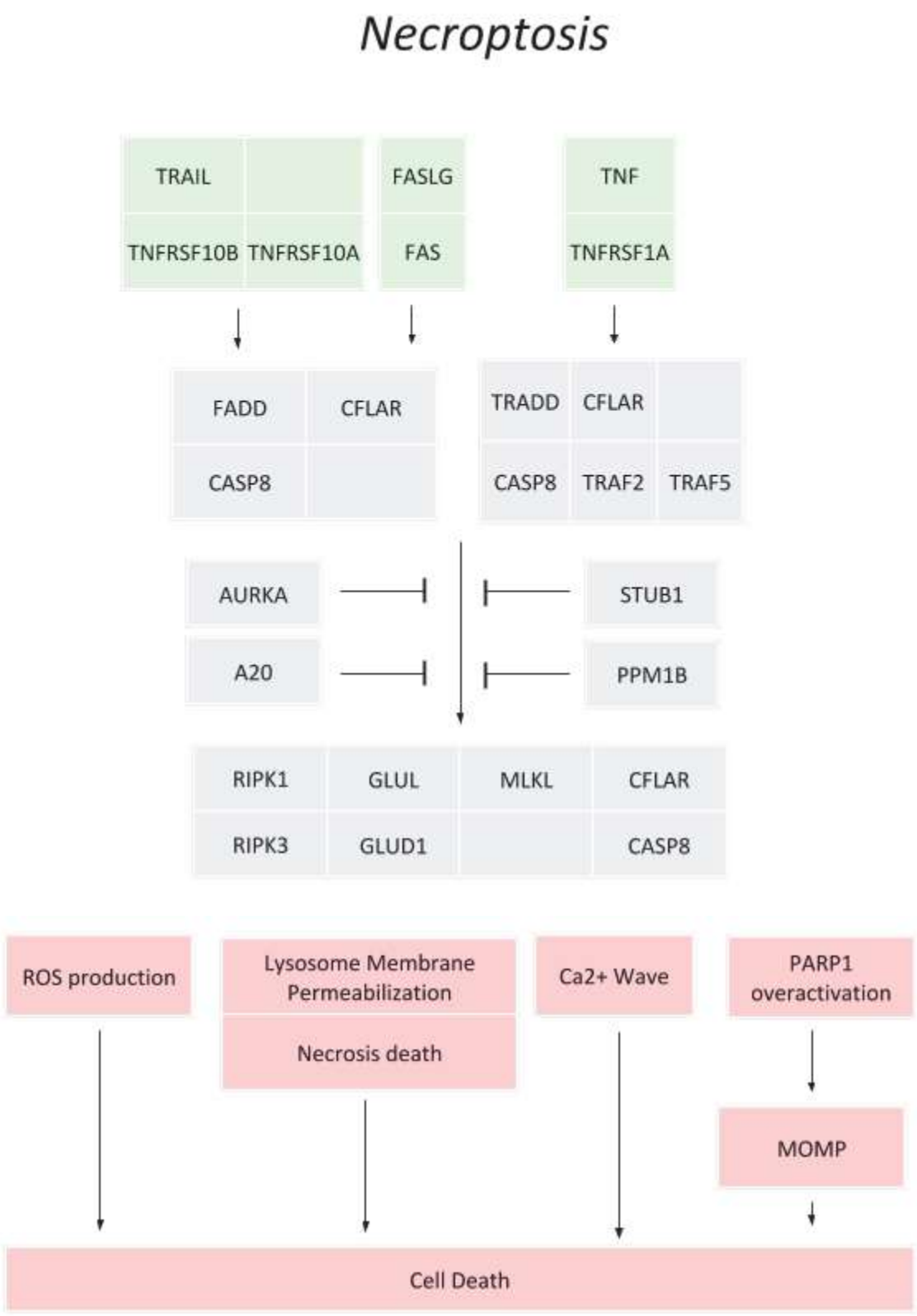

Supplemental Figure 3C

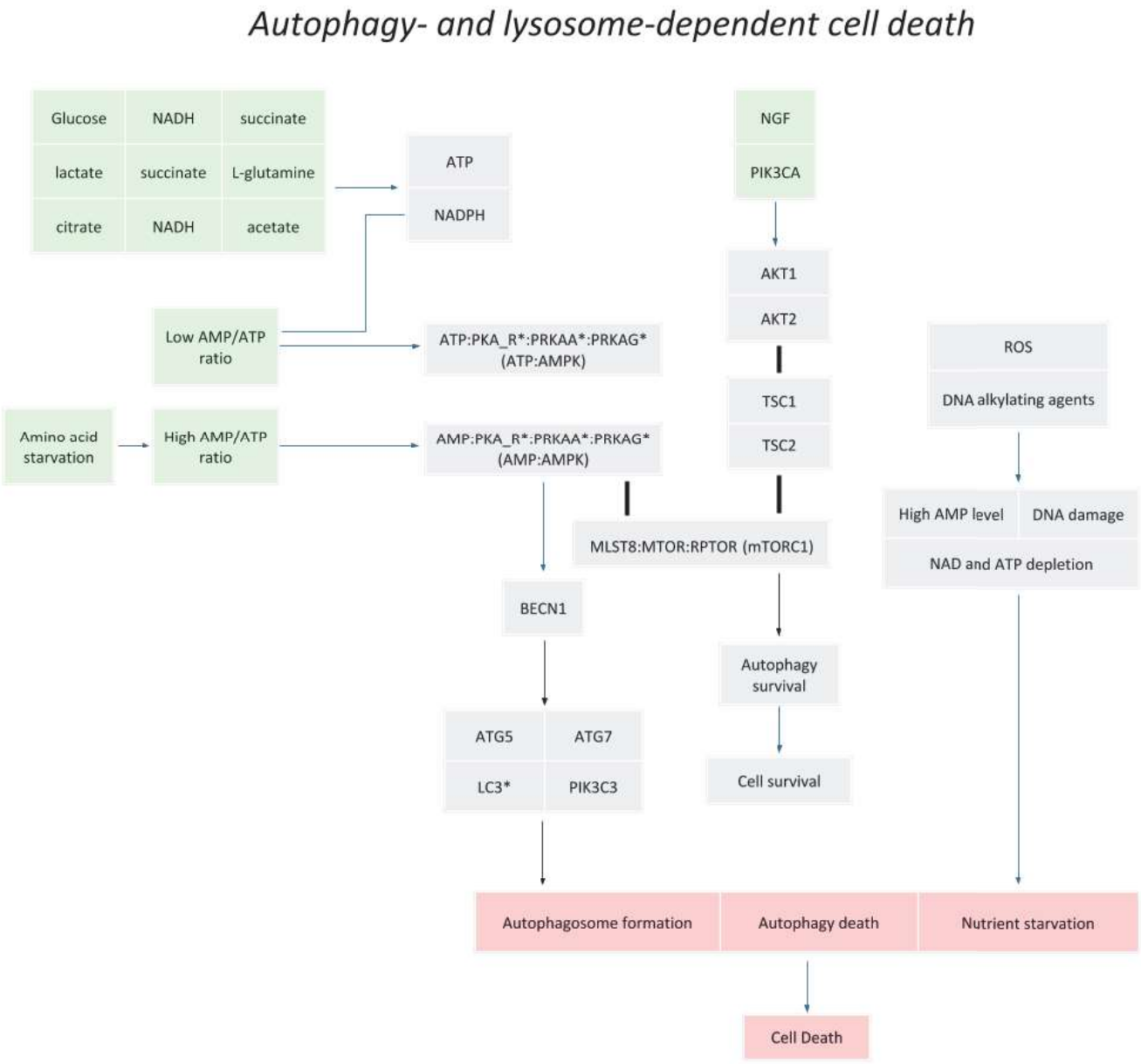

Supplemental Figure 3D

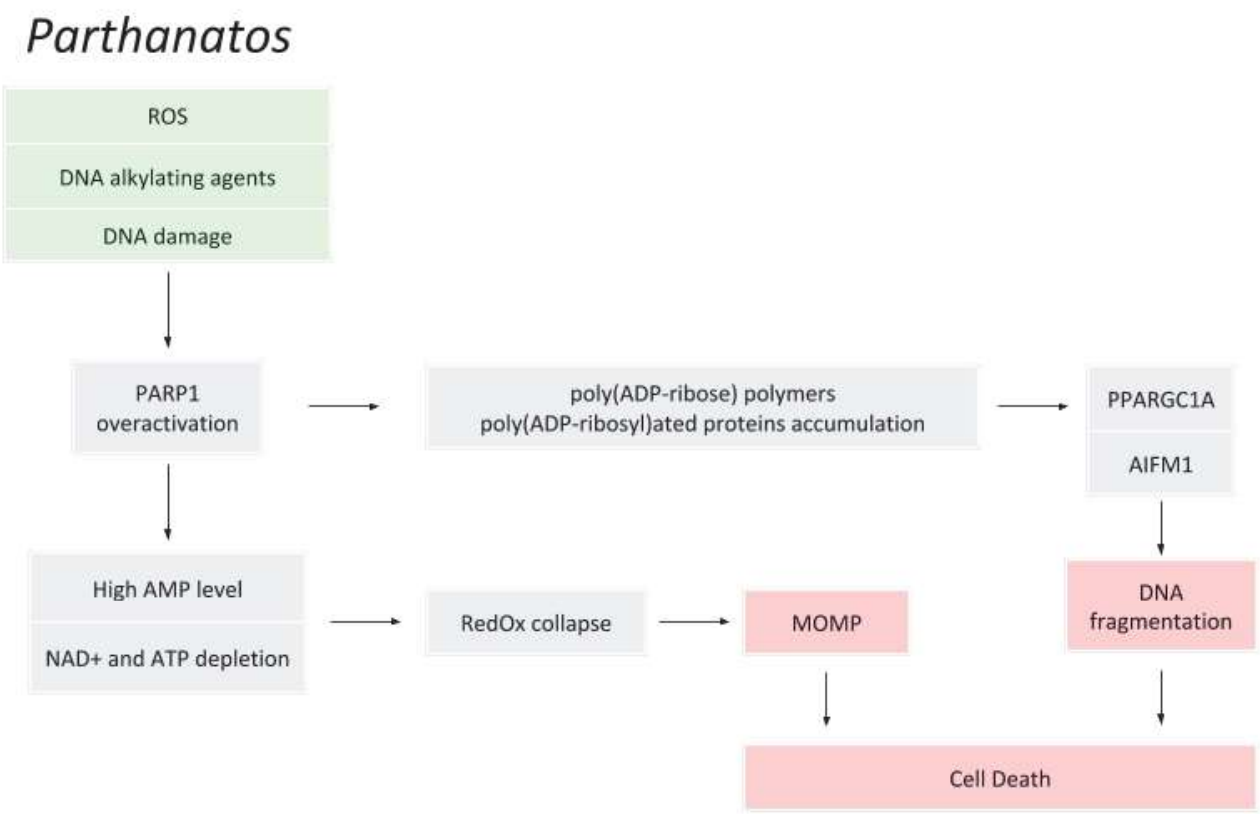

Supplemental Figure 3E-G

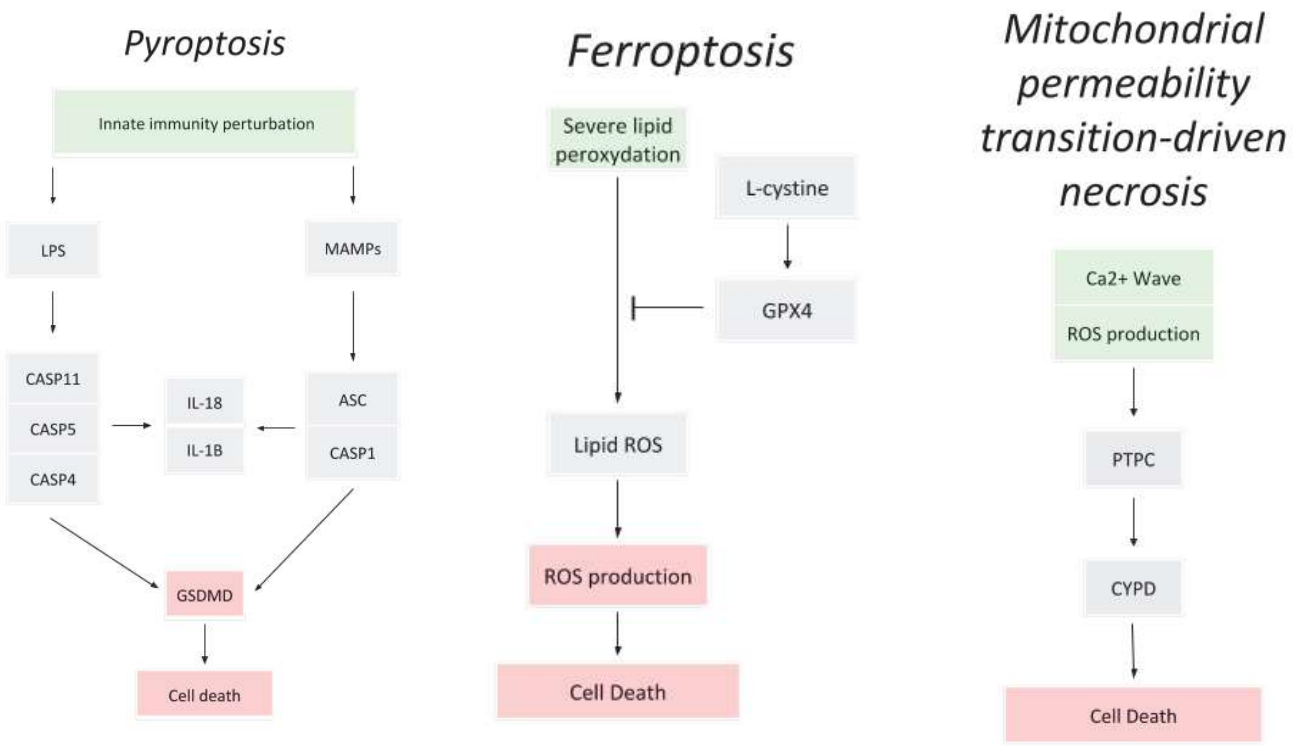

Supplemental Figure 4

A

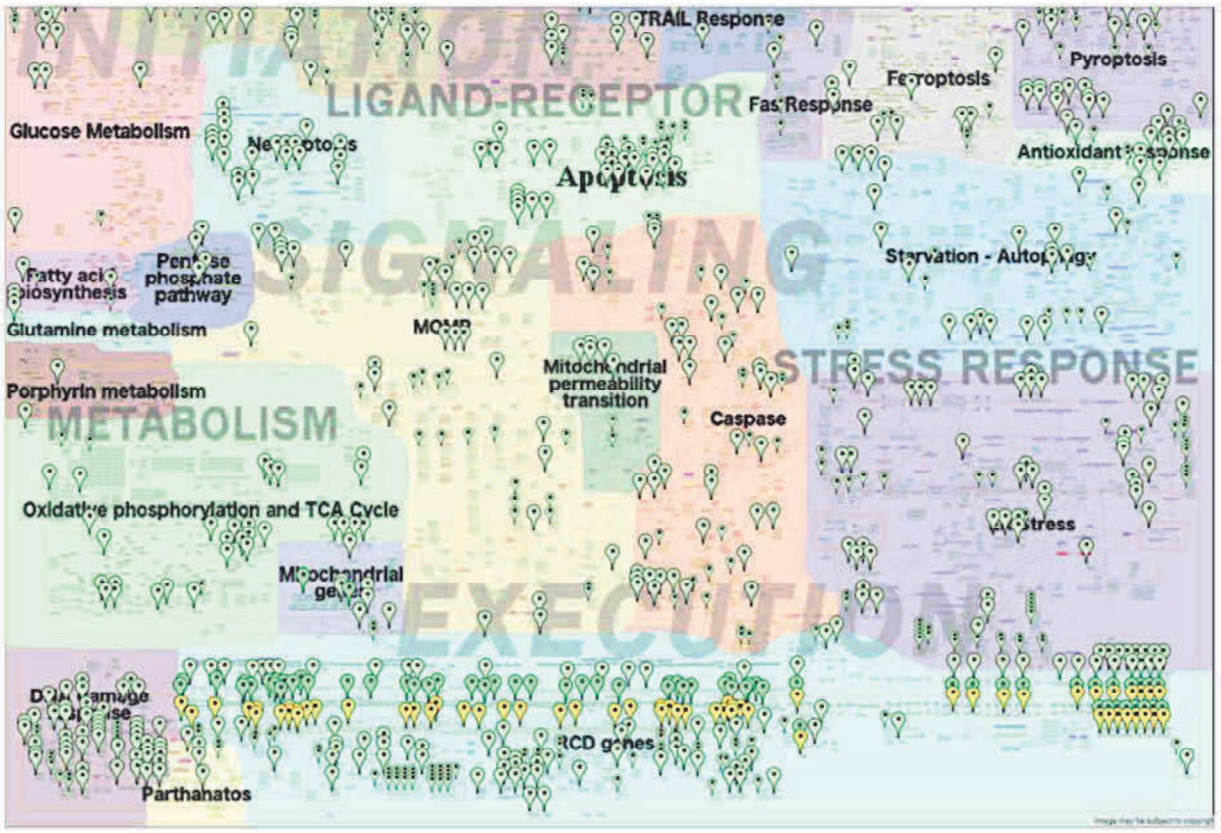

B

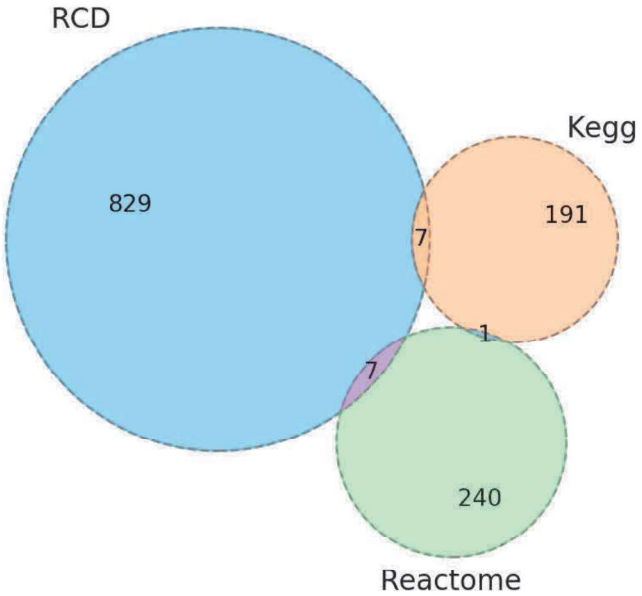

Supplemental Figure 5

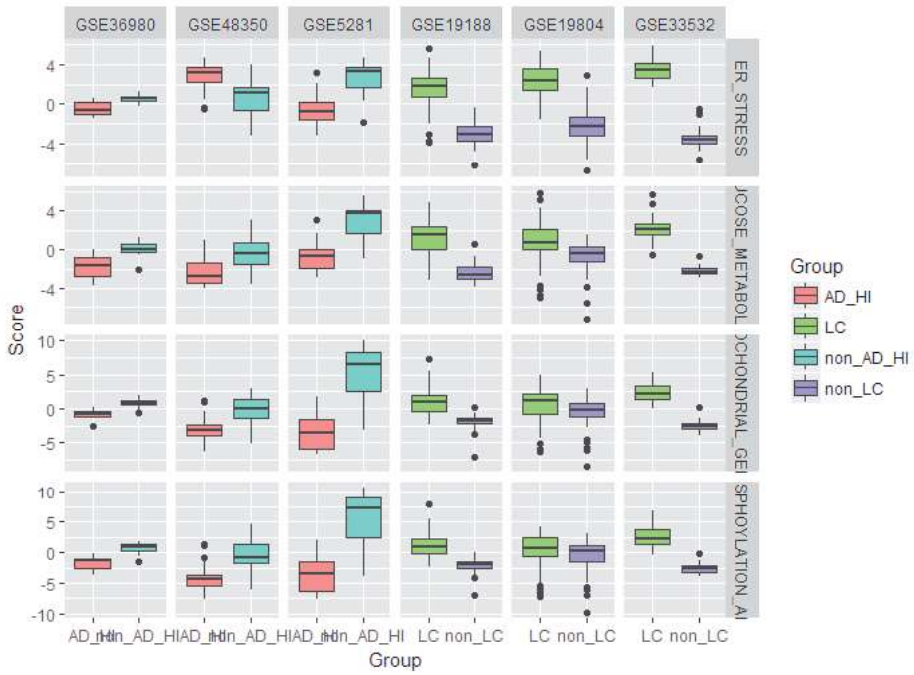

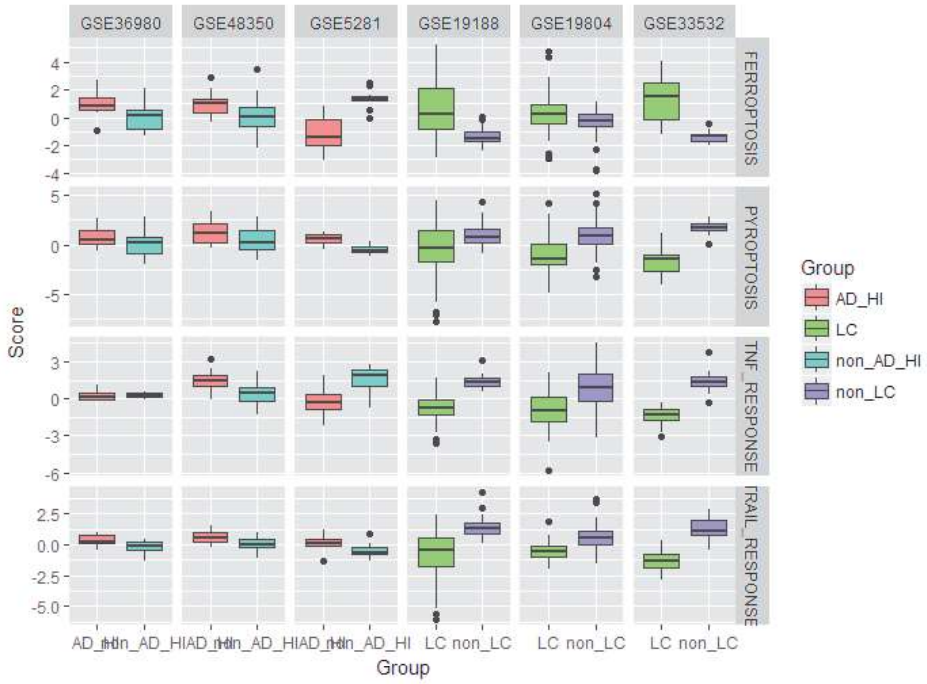

Supplemental Figure 6

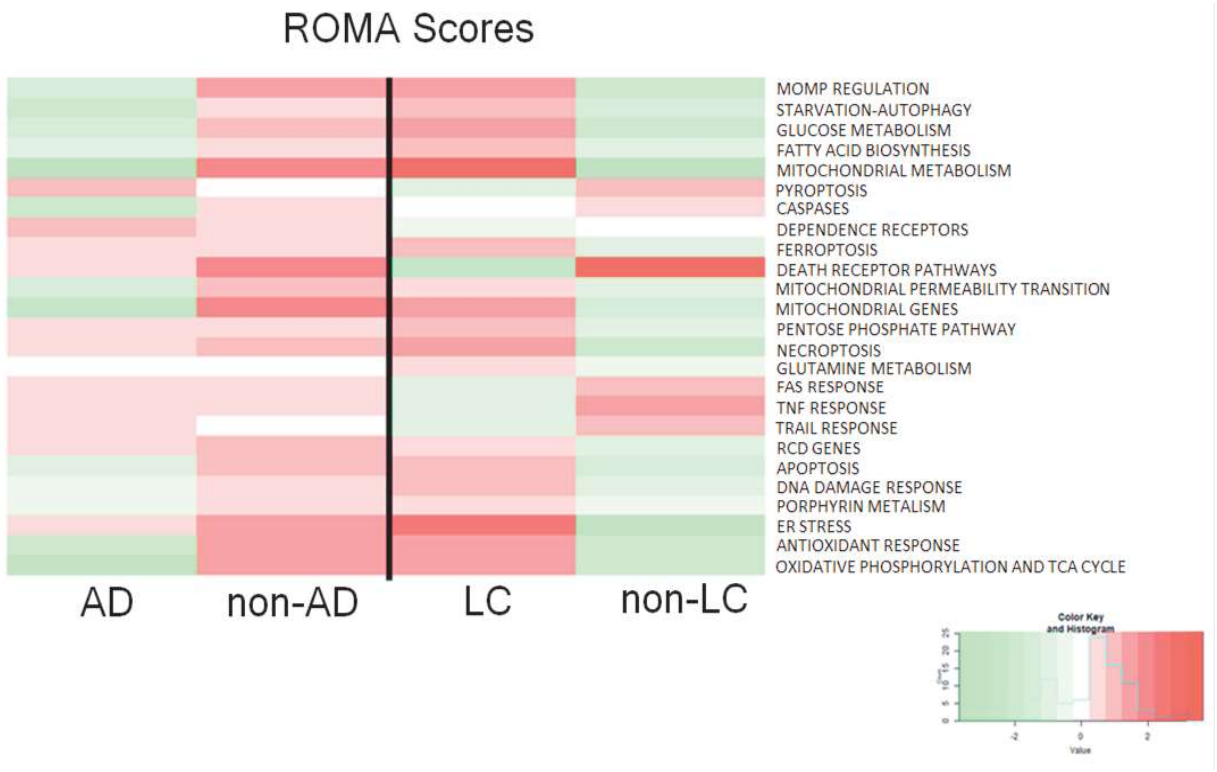

Supplemental table 1

	Input		
Initiation (reversible)			
Ligand-Receptor			
Death receptor			
Trail response	TRAIL	TNFRSF10B	TNFRSF10A
Fas = CD95 response	FAS		
TNF response	TNF	TNFRSF1A	
Dependence receptor			
Metabolism			
General metabolism			
Glucose metabolism	Glucose	lactate	
Fatty acid biosynthesis	citrate	coenzyme A	
Pentose phosphate pathway	glucose-6P	ribulose-5P	
Glutamine metabolism	L-glutamine	GLUL	L-glutamate
Porphyrin metabolism	succinyl-CoA	glycine	
Mitochondrial metabolism			
Oxidative phosphorylation	NADH	O2	
TCA cycle	succinate	L-glutamine	citrate
Mitochondrial genes	MT-DNA		
Stress response			
DNA damage response	DNA damage	PPARGC1A	AIFM1
Antioxidant response	ENOS*	HIFA	O2
ER stress	unfolded protein	ITPR*	IRE1-alpha*
Starvation - Autophagy	MTOR	AKT*	AMPK
Signalling (switchrable)			
Apoptosis	BAD	BCL2	BAX
Necroptosis	RIPK1	RIPK3	MLKL
Ferroptosis	Fe3+	L-cystine	GPX*
Parthanatos	ROS	DNA alkylating agents	
Pyroptosis	ROS Production	LF*	Flagellin*
Execution (irreversible)			
MOMP	BAD	BCL2	BAX
Mitochondrial permeability transition	ROS Production	Ca2+ Wave	
Caspases	Caspase 9*	Caspase 8*	Caspase 10*
RCD genes	active NRF*	p53*	E2F1

	CFLAR			
acetate	NAD+			
DNA2	MDC1	p53*		
ferroheme b	bilirubin	ROS	PRDX*	GSH
PERK	amino acid starvation	viral infection	Heme deficiency	
ROS Production	Hypoxia	LC3*	BECN1	active Caspases*
BAK1	Cytochrome_c*	Caspase8*	Caspase10*	
GLUL	GLUD1	PGAM5		
NLRC4	NLRP3	AIM2	Pyrin*	RHO
BAK1	Cytochrome_c*			
HIH1A	NFKB1	MYC	DNA damage	

Output		
cleaved Caspase8*	cleaved Caspase 10*	MLKL
cleaved Caspase8*	cleaved Caspase 10*	MLKL
cleaved Caspase8*	cleaved Caspase 10*	MLKL
Lipid synthesis	Biomass production	
RNA	DNA2	xylulose-5P
L-glutamine	Autophagy survival	
heme	ferroheme b	
ATP		
NADPH		
Mitochondrial DNA damage		
DNA integrity	DNA fragmentation	Apoptotic death
biliverdin	GSSG	mitochondrial damage
apoptosis	ER Stress	Persistant ER Stress
Low AMP/ATP ratio	High AMP/ATP ratio	Necrosis death
MOMP	ROS production	active Caspases*
ROS Production	Necrosis death	Lysosome Membrane Permeabilization
Lipid ROS	ROS	Ferroptosis
PARP1 overactivation	High AMP level	DNA damage
Pyroptosis		
MOMP	ROS production	
MOMP	PTPC	ROS production
Apoptotic death	cleaved Caspase 3*	cleaved Caspase7*

DAXX	Apoptotic death	Necrosis death	Cell survival
DAXX	Apoptotic death	Necrosis death	Cell survival
DAXX	Apoptotic death	Necrosis death	Cell survival

RIDD process	Cell death	Cell survival	
Autophagosome formation	Autophagy survival	Autophagy death	Nutrient starvation

Apoptotic death	cleaved Caspase8*	cleaved Caspase 10*	APOPTOSOME
Ca2+ Wave	PARP activation		
Cell death	NAD and ATP depletion		

cleaved BCL2*	cleaved MCL1*	cleaved BAK*

Input	Output
TRAIL	cleaved Caspase8*
TNFRSF10B	cleaved Caspase 10*
TNFRSF10A	MLKL
FAS	DAXX
TNF	Apoptotic death
TNFRSF1A	Necrosis death
CFLAR	Cell survival
Glucose	Lipid synthesis
lactate	Biomass production
citrate	RNA
coenzyme A	DNA2
glucose-6P	xylulose-5P
ribulose-5P	L-glutamine
L-glutamine	Autophagy survival
GLUL	heme
L-glutamate	ferroheme b
succinyl-CoA	ATP
glycine	NADPH
NADH	Mitochondrial DNA damage
O2	DNA integrity
succinate	DNA fragmentation
acetate	biliverdin
NAD+	GSSG
MT-DNA	mitochondrial damage
DNA damage	apoptosis
PPARGC1A	ER Stress
AIFM1	Persistant ER Stress
DNA2	RIDD process
MDC1	Cell death
p53*	Low AMP/ATP ratio
ENOS*	High AMP/ATP ratio
HIFA	Autophagosome formation
ferroheme b	Autophagy death
bilirubin	Nutrient starvation
ROS	MOMP
PRDX*	ROS production
GSH	active Caspases*
unfolded protein	APOPTOSOME
ITPR*	Lysosome Membrane Permeabilization
IRE1-alpha*	Ca2+ Wave
PERK	PARP activation
amino acid starvation	Lipid ROS
viral infection	ROS
Heme deficiency	Ferroptosis
MTOR	PARP1 overactivation
AKT*	High AMP level

AMPK
ROS Production
Hypoxia
LC3*
BECN1
active Caspases*
BAD
BCL2
BAX
BAK1
Cytochrome_c*
Caspase8*
Caspase10*
RIPK1
RIPK3
MLKL
GLUD1
PGAM5
Fe3+
L-cystine
GPX*
DNA alkylating agents
LF*
Flagellin*
NLRC4
NLRP3
AIM2
Pyrin*
RHO
Ca2+ Wave
Caspase 9*
Caspase 8*
Caspase 10*
active NRF*
E2F1
HIH1A
NFKB1
MYC

DNA damage
NAD and ATP depletion
Pyroptosis
PTPC
cleaved Caspase 3*
cleaved Caspase7*
cleaved BCL2*
cleaved MCL1*
cleaved BAK*

Supplementary Table 2 : Comparison of gene content between pathways from KEGG and REACTOME databases to the Regulated Cell Death map. HUGO names were used as common IDs.

HUGO names - based count: KEGG						
KEGG - pathway	**RCD corresponding module**	**KEGG**	**ACSN**	**Common with ACSN**	**Not present in ACSN**	**Not present in KEGG**
Master map	_Master map	956	891	423	533	468
Glutathione metabolism	ANTIOXIDANT RESPONSE	54	161	6	48	155
Apoptosis	APOPTOSIS	137	221	50	87	171
Fatty acid biosynthesis	FATTY ACID BIOSYNTHESIS	13	42	3	10	39
Ferroptosis	FERROPTOSIS	40	34	13	27	21
Glycolysis Gluconeogenesis	GLUCOSE METABOLISM	68	106	30	38	76
Glutamate metabolism	GLUTAMINE METABOLISM	4	20	4	0	16
Citrate cycle (TCA cycle)	OXIDATIVE PHOSPHORYLATION AND TCA CYCLE	30	185	22	8	163
Oxidative phosphorylation	OXIDATIVE PHOSPHORYLATION AND TCA CYCLE	133	185	69	64	116
Pentose phosphate pathway	PENTOSE PHOSPHATE PATHWAY	30	18	0	30	18
Porphyrin and chlorophyll metabolism	PORPHYRIN METABOLISM	42	18	11	31	7
HIF-1 signalling pathway	RCD GENES	100	137	17	83	120
p53 signalling pathway	RCD GENES	68	137	17	51	120
mTOR signalling pathway	STARVATION-AUTOPHAGY	151	167	34	117	133
Autophagy - animal	STARVATION-AUTOPHAGY	128	167	65	63	102
Necroptosis	NECROPTOSIS + TNF RESPONSE + TRAIL RESPONSE + FAS RESPONSE	165	154	52	113	102
TNF signalling pathway	TNF RESPONSE + NECROPTOSIS + APOPTOSIS	108	306	44	64	262

HUGO – based count: Reactome						
Reactome pathway	**RCD corresponding module**	**Reactome**	**ACSN**	**Common with ACSN**	**Not present in ACSN**	**Not present in Reactome**
Master map	_Master map	809	891	323	486	568
Death Receptor Signalling	DEATH RECEPTOR PATHWAYS	54	249	29	25	220
Unfolded Protein Response	ER STRESS	159	148	41	118	107
Fatty acid metabolism	FATTY ACID BIOSYNTHESIS	179	42	8	171	34
Xylulose	GLUCOSE METABOLISM	6	106	0	6	106
Glucose metabolism	GLUCOSE METABOLISM	96	106	33	63	73
Glutamine metabolism	GLUTAMINE METABOLISM	2	20	2	0	18
TCA cycle and oxidative phosphorylation	OXIDATIVE PHOSPHORYLATION AND TCA CYCLE	169	185	111	58	74
Pentose phosphate pathway	PENTOSE PHOSPHATE PATHWAY	15	18	0	15	18
Metabolism of porphyrins	PORPHYRIN METABOLISM	17	18	11	6	7
mTOR signalling	STARVATION-AUTOPHAGY	40	167	24	16	143
Programmed Cell Death	APOPTOSIS + NECROPTOSIS	178	284	49	129	235

Supplemental table 3

Table 3. Genes corresponding to copy number average equal or larger than 4 in the groups of ovarian cancer cases.

Differentiated		Immunoreactive		Mesenchymal		Proliferative	
Genes	*Average*	*Genes*	*Average*	*Genes*	*Average*	*Genes*	*Average*
CYC1	4.63	ACER3	4.06	BIRC7	4.09	ACSS1	4.24
DEPTOR	4.68	APH1A	4.12	COX6C	4.05	ACSS2	4.43
DERL1	4.68	ARNT	4.12	CYC1	4.67	AIM2	4.14
GPT	4.63	COX6C	4.19	DEPTOR	4.52	APH1A	4.19
GRINA	4.63	CREB3L4	4.06	DERL1	4.67	ARNT	4.19
MYC	4.79	CTSS	4.12	GPT	4.67	ATF6	4.19
NDRG1	4.84	CYC1	4.25	GRINA	4.52	ATP5C1	4.05
NDUFB9	4.68	DEPTOR	4.31	MIR1.1	4.19	ATP5E	4.48
SLC2A2	4.10	DERL1	4.37	MIR133A2	4.19	BCL2L1	4.76
TNFRSF11B	4.53	EIFB5	4.00	MYC	4.81	BIRC7	4.48
TNFSF10	4.05	GPT	4.25	NDRG1	4.81	C12orf5	4.38
WISP1	4.84	GRINA	4.25	NDUFB5	4.05	CDKN1B	4.24
		MCL1	4.12	NDUFB9	4.71	COX4I2	4.76
		MYC	4.56	PIK3CA	4.09	CREB3L4	4.19
		NDRG1	4.50	RRM2B	4.05	CSE1L	4.29
		NDUFB5	4.19	SLC2A2	4.00	CSNK2A1	4.48
		NDUFB9	4.37	TNFRSF11B	4.57	CTSS	4.19
		NDUFC2	4.25	TNFSF10	4.00	DNAJB11	4.86
		NDUFS5	4.00	WISP1	4.86	DNM1L	4.24
		NDUFS6	4.06	YWHAZ	4.05	DUSP16	4.33
		PAK1	4.06			E2F1	4.48
		PIK3CA	4.18			E2F3	4.00
		RRM2B	4.25			EGLN1	4.00
		SDHA	4.00			EIF2AK2	4.00
		SLC2A2	4.50			EIF2B4	4.00
		TFRC	4.00			EIF2B5	4.71
		TNFRSF11B	4.31			EIF2S2	4.48
		TNFSF10	4.44			ENO2	4.48

	TRIT1	4.06		FAIM	4.05
	WISP1	4.50		FASLG	4.05
	YWHAZ	4.12		FBXO45	4.48
				FH	4.14
				FLAD1	4.19
				GABARAPL1	4.33
				GAPDH	4.43
				GLUL	4.09
				GSS	4.43
				H2AFJ	4.29
				HAX1	4.19
				HIST2H2AC	4.19
				IDH3B	4.38
				ING4	4.43
				ITCH	4.48
				ITPR2	4.48
				KIAA0226	4.478
				LDHB	4.19
				LMNA	4.24
				MAP1LC3A	4.48
				MCL1	4.19
				MIR1.1	4.48
				MIR133A2	4.48
				MIR16.2	4.43
				MIR199A2	4.09
				MIR214	4.09
				MIR23A	4.09
				MYC	4.14
				NCF2	4.09
				NDUFA9	4.38
				NDUFB5	4.81
				NDUFB7	4.33

			NDUFB9	4.09
			NDUFS2	4.19
			NFE2L2	4.00
			NLRP3	4.33
			NME7	4.09
			PFKFB3	4.09
			PIK3CA	4.86
			PKLR	4.24
			PLA2G4A	4.00
			PPOX	4.19
			PRKAB2	4.29
			PRKACA	4.14
			RNF168	4.48
			RYR2	4.24
			SDHC	4.19
			SHC1	4.19
			SLC2A2	4.86
			SLC2A3	4.38
			SRXN1	4.43
			TFB2M	4.29
			TFRC	4.48
			TNFRSF1A	4.29
			TNFSF10	4.86
			TPI1	4.43
			TRIB3	4.48
			TRPC1	4.14
			TXNIP	4.14
			UQCRFS1	4.00
			YWHAB	4.24